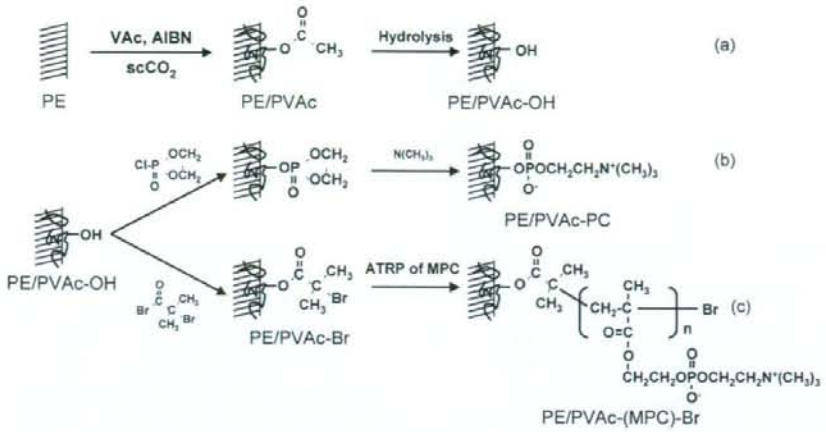

Fig. 1. Synthetic route of poly(MPC)-grafted polymer composite through SI-ATRP.

acetate) (PVAc) by *in situ* polymerization of vinyl acetate in the PE substrate by using supercritical carbon dioxide ($scCO_2$) fluid [20,21]. Further, we converted the acetyl groups in PVAc on the surface of the polymer composite to hydroxyl groups following the PC groups (Fig. 1(a) and (b)). In this way, the surface prepared by two-dimensional (2D) correction in which the PC group was anchored directly on the surface of the polymer composite suppressed effectively the protein adsorption. It is expected that new polymer biomaterials could be created by the new method that is the surface modification of polymer composite prepared by $scCO_2$.

In this study, the biocompatible surface was constructed by three-dimensional (3D) modification, that is, the phospholipid polymer was grafted from the surface of the polymer composite by SI-ATRP of MPC. The surface initiator was immobilized by the reaction between 2-bromoisobutyryl bromide and the hydroxyl group on the polymer composite surface. Subsequently, graft polymerization of MPC was carried out by the SI-ATRP method (Fig. 1(c)). We reported the 3D-controlled poly(MPC)-grafted surface on the PE/PVAc polymer composite. Further, we discussed that the effect of the poly(MPC) chain length on the surface properties and protein adsorption behavior compared with those of PC group directly immobilized surface.

2. Experiment

2.1. Materials

PE/PVAc, PE/PVAc-OH, and PE/PVAc-PC were synthesized and purified by a method reported previously [20,21], as shown in Fig. 1(a) and (b). 2-Bromoisobutyryl bromide, 2,2′-bipyridyl (Bpy), ethyl-2-bromoisobutyrate, copper(I) bromide (CuBr), and fluorescein isothiocyanate-labeled bovine serum albumin (FITC–BSA) were purchased from Sigma–Aldrich Co., Saint Louis, USA, and used as-received. The other reagents were purified by conventional distillation.

2.2. Preparation of poly(MPC)-grafted polymer composite: PE/PVAc-(MPC)-Br

On the surface of PE/PVAc-OH, 2-bromoisobutyryl bromide was reacted to introduce the initiator of SI-ATRP (PE/PVAc-Br). Argon gas was purged in methanol to eliminate oxygen before the polymerization. MPC (0.01 mol) was added to the Schlenk flask containing a magnetic stir bar and was subsequently dissolved in 10 mL of methanol bubbled with argon for 15 min to eliminate oxygen. CuBr and Bpy were added to the MPC solution with stirring under argon. After being stirred for 30 min under an argon gas atmosphere, the PE/PVAc-Br plate was submerged to the flask. Ethyl-2-bromoisobutyrate was then added as a sacrificial initiator ([I]). The graft polymerization was performed at 25 °C with stirring under an argon gas atmosphere. After 24 h, the poly(MPC)-grafted polymer composite (PE/PVAc-(MPC)-Br) plate was removed from the polymerization mixture and rinsed with methanol and water. Subsequently, the PE/PVAc-(MPC)-Br plate was dried *in vacuo* at room temperature after being extracted with methanol for 24 h to remove the unreacted reagents and homopolymer by using a Soxhlet-extractor. Four different [MPC]/[I] ratios, 50, 100, 150, and 200, were applied to prepare poly(MPC)-grafted polymer composites with different poly(MPC) chain lengths (MPC monomer units). The polymerization condition is as follows: [MPC] = 1.0 M, [CuBr]:[Bpy]:[I] = 1:2:1.

The molecular weight of free poly(MPC) in solution was measured by gel permeation chromatography (GPC) using a Shodex SB-804HQ column (upper limit of the molecular weight was $\sim 1.0 \times 10^7$ g/mol, the flow rate was 0.40 mL/min).

Surface characterizations of the sample were carried out by X-ray photoelectron spectroscopy (XPS) (AXIS-HSi, Shimadzu/KRATOS, Kyoto, Japan), dynamic water contact angle (DCA) measurement (CA-W, Kyowa Interface Science Co., Tokyo, Japan), and atomic force microscopy (AFM) (NanoScope IIIa Multimode SPM, Veeco Instruments, Tokyo, Japan).

2.3. Protein adsorption test

Polymer composites with poly(MPC)-grafted surface were exposed to 4.5 mg/mL FTIC-BSA in Dulbecco's phosphate-buffered saline (PBS) at 37 °C for 60 min and then rinsed five times with fresh PBS. The FITC–BSA concentration was 10% of the plasma concentration. The sample was dried in an argon stream and observed with a fluorescence microscope. The relative fluorescent intensity based on the adsorbed protein on the surface was calculated by comparison with the adsorbed protein on the unmodified PE surface.

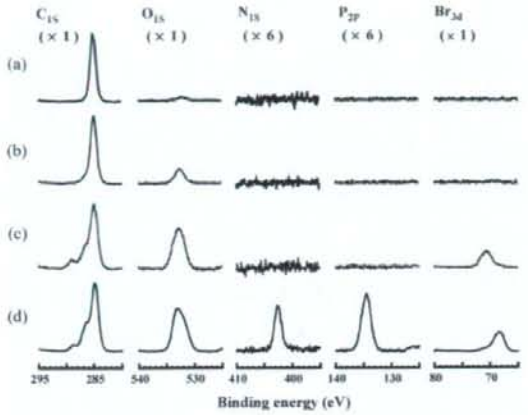

Fig. 2. XPS charts of (a) unmodified PE, (b) PE/PVAc-OH, (c) PE/PVAc-Br, and (d) PE/PVAc-(MPC)-Br ([MPC]/[I] = 100). The intensities of each atom were normalized by the intensity of C 1s at 285 eV.

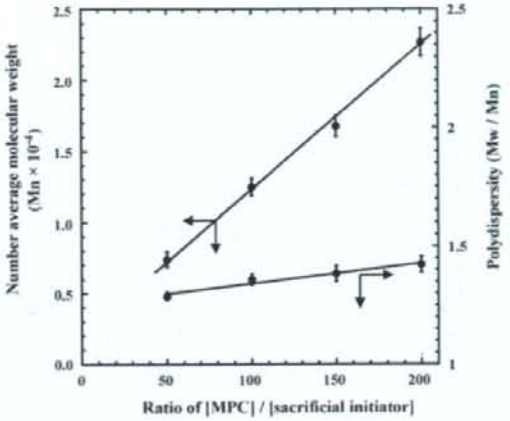

Fig. 3. Relationship between [MPC]/[sacrificial initiator] values and molecular weight of the poly(MPC) formed.

3. Results and discussion

3.1. Preparation of poly(MPC)-grafted polymer composite

Fig. 2 shows the XPS charts of unmodified PE, PE/PVAc-OH, PE/PVAc-Br and PE/PVAc-(MPC)-Br. In the unmodified PE, a strong intensity was observed at 285 eV (Fig. 2(a)). This is attributed to the carbon atoms in the methylene chain. The XPS peaks of PE/PVAc-OH broadened in the C 1s region and new peaks corresponding to the hydroxyl group were observed in the O 1s region (Fig. 2(b)). After the immobilization of the ATRP initiator on the polymer composite (Fig. 2(c)), the XPS peaks became broad in the C 1s region, the peak intensity of the O 1s region increased and the new peak was observed in the Br 3d region. This broad peak was attributed to the 2-bromoisobutyl groups in the C 1s region. An increase in the intensity of the O 1s region and the new peak in the Br 3d region were attributed to the carbonyl group (C=O) and bromine on the 2-bromoisobutyl groups, respectively. After the grafting of poly(MPC) (Fig. 2(d)), the increase in the peak intensity is caused by the increase in the amount of oxygen in the O 1s region, moreover, the nitrogen and phosphorus peaks were observed at 403 eV and 134 eV, respectively, and these peaks were attributed to the PC groups. In addition, the position of the bromine peak was shifted from a binding energy of 71–69 eV by the SI-ATRP of MPC monomer. These results confirmed that the surface initiator for the SI-ATRP was immobilized on the PE/PVAc polymer composite and the SI-ATRP of MPC succeeded had been successfully performed.

In this study, we added ethyl-2-bromoisobutyrate ([I]) as the sacrificial initiator to the polymerization solution to provide a deactivator that was concentration sufficiently high for the control of ATRP grafting from the surface of PE/PVAc-Br. The added sacrificial initiator also facilitated the control of the polymer chain length through the variation of the [MPC]/[I] ratio, assuming that the chains grown from the surface and in solution have similar molecular weights. This assumption was proved to be valid for the PMMA-grafted PE films [22]. Figs. 3 and 4 show the relationship between the molecular weight of poly(MPC) and the atomic surface composition with the [MPC]/[I] ratio, respectively. The number average of the molecular weight (Mn) of poly(MPC) and the phosphorus composition (P 2p/C 1s ratio determined by XPS) increased linearly with the [MPC]/[I] ratio, suggesting that the

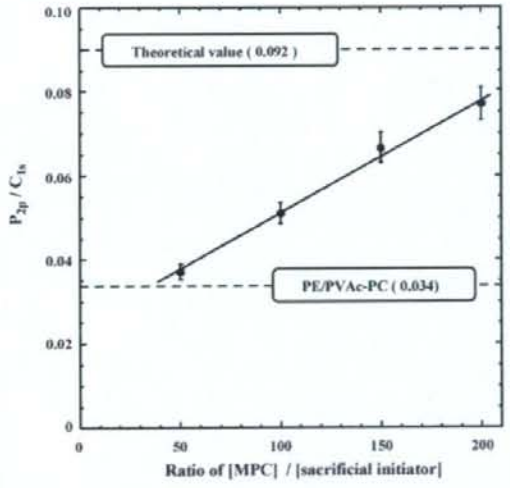

Fig. 4. Relationship between [MPC]/[sacrificial initiator] values and P 2p/C 1s values determined by XPS analysis.

ATRP grafting of MPC from the polymer composite surface was well-controlled process. In addition, the value of the P 2p/C 1s ratio approaches the theoretical value (0.092) as the chain length of poly(MPC) increases. This fact indicates that the density of the PC group on the surface increases with the chain length of the grafted poly(MPC). Further, the value of the P 2p/C 1s ratio of PE/PVAc-PC (0.034) was almost the same in the case of small graft chain lengths ([MPC]/[I] = 50). In this case, it is thought that the poly(MPC)-grafted surface ([MPC]/[I] = 50) and PE/PVAc-PC have similar surface properties.

3.2. Contact angle measurements

Dynamic water contact angle measurement has commonly been used to characterize the relative hydrophilicity or hydrophobicity of surfaces [23]. For surfaces with comparable structures, a relatively low contact angle value generally implies high

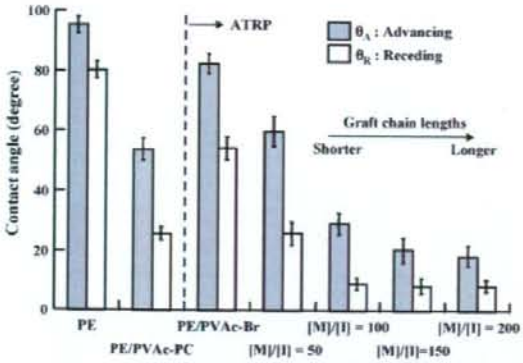

Fig. 5. Advancing and receding water contact angles of poly(MPC)-grafted surfaces of the polymer composite.

hydrophilicity. Fig. 5 shows the results of the DCA measurements. The advancing (θ_A) and receding (θ_R) contact angles decreased with the introduction of PC groups on the surface. Moreover, the poly(MPC)-grafted surface ([MPC]/[I] = 50) and PE/PVAc-PC with almost the same surface composition exhibited similar hydrophilicity. In the case of large graft-chain lengths, the hydrophilicity of the surface increased considerably. PE/PVAc-OH caused a hydrophilic/hydrophobic microphase separation because the surface of PE/PVAc assumed a microdomain structure comprising of crystalline of PE and amorphous regions (PE and PVAc amorphous) [21]. The surface initiator could be introduced only in hydroxyl groups generated in the hydrophilic domain based on the PVAc, and MPC could be polymerized from the domain by introducing the surface initiator. Therefore, the short poly(MPC)-grafted chains did not cover the hydrophobic domain based on PE; however, the long graft chains could cover the hydrophobic domain. Thus, the hydrophilicity of the polymer composite surfaces was greatly improved by the introduction of the poly(MPC) graft. Consequently, we inferred that the surface density of the PC groups considerably influences the surface properties and 3D modification is preferred to 2D modification, which is achieved by the direct immobilization of PC groups.

3.3. Surface morphology

The wet condition topology of the surfaces was examined by employing fluid tapping mode AFM in pure water. Fig. 6 shows height images of the unmodified PE and grafted poly(MPC) surfaces. The unmodified PE surface was smooth with a root mean square (RMS) roughness of 1.60 nm. The surface of the introduced surface initiator had an RMS roughness of 4.78 nm (Fig. 6(d)–(f)) indicate that the morphology of poly(MPC)-grafted surface was dependent on the poly(MPC) chain length. The surface containing chains with small lengths showed a greater roughness (Fig. 6(e)) as compared to the surfaces comprising chains with large lengths (Fig. 6(f)), as is evident from the RMS data. Further, on the surface of longer chain length ([MPC]/[I] = 100), regular peaks and valleys were observed within the measurement areas. These results indicated that the surface was covered with long poly(MPC)-graft chains.

3.4. Protein adsorption test

Fig. 7 shows the fluorescent intensity of the FITC–BSA adsorbed on the surfaces. The fluorescent intensity is proportional to the amount of adsorbed protein on the surface. The amount of the FITC–BSA adsorbed on the surface was in good agreement with the contact angle with water depended on the density of the PC groups, as shown in Fig. 5. The PC group immobilized surface effectively reduced protein adsorption as compared with unmodified PE; further, the amount of protein adsorbed on the poly(MPC)-grafted surface decreased with an increase in the chain length of poly(MPC). Both the hydrophilicity and surface morphology are significant factors for the protein adsorption resistance properties. The suppression of protein adsorption by the poly(MPC)-grafted surface was considerably greater than that on PE/PVAc-PC because of the higher density of PC groups. The amount of protein adsorbed on the poly(MPC)-grafted surface decreased with an increase in the chain length of grafted poly(MPC). We determined the amount of adsorbed BSA on the unmodified PE and PE/PVAc-PC surface quantitatively and it was 1.12 $\mu g/cm^2$ and 0.22 $\mu g/cm^2$, respectively [20]. The value obtained on the PC group immobilized surface was sufficient to suppress thrombus formation even when the surface was in contact with blood [24]. Thus, such significant reduction in protein adsorption that was observed in the case of

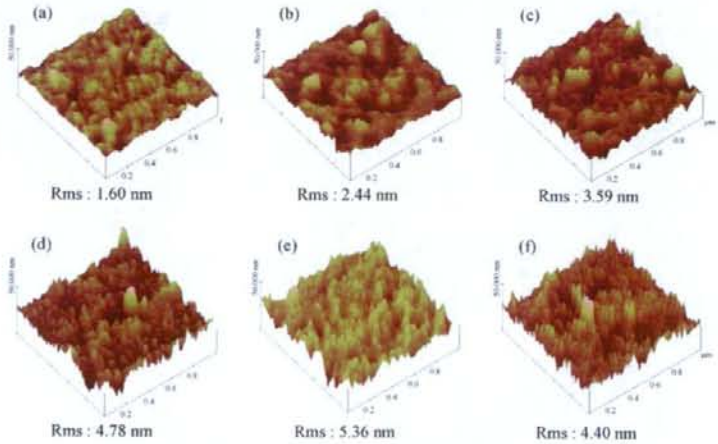

Fig. 6. AFM 3D height images of (a) unmodified PE, (b) PE/PVAc-OH, (c) PE/PVAc-PC, (d) PE/PVAc-Br, (e) PE/PVAc-(MPC)-Br ([MPC]/[I] = 50), and (f) PE/PVAc-(MPC)-Br ([MPC]/[I] = 100) (image size: 1 μm × 1 μm × 50 μm).

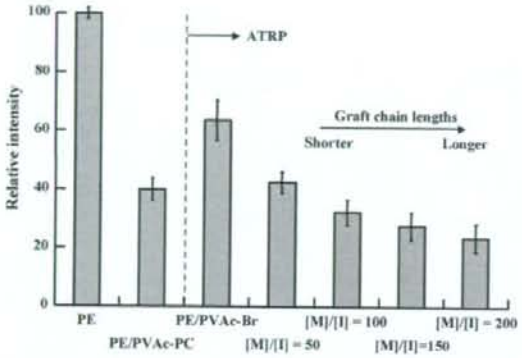

Fig. 7. Relative fluorescence intensity based on the FITC–BSA adsorbed on the various surfaces.

the poly(MPC)-grafted surface may be good for the inhibition of thrombus formation. Therefore, the 3D regulated aliment of PC groups on the surface of the polymer composite has excellent potential in the fabrication of biomedical devices.

4. Conclusion

The surface modification of polyolefins such as PE is very difficult because of these low surface tension and chemical stability. If the grafts are covalently attached to the substrate, the modified layer is stable and does not delaminate. To prepare for the biocompatible surface, phospholipid moieties were directly anchored on the new polymer composite with hydroxyl groups on the surface through the surface reaction of hydroxyl groups. Two different procedures such as 2D modification and 3D modification were applied to obtain the steady biocompatible surface. Our previous article demonstrated the 2D modification that PC groups were directly anchored on the surface of the polymer composite. In this study, we have reported a versatile approach that is 3D modification for preparing poly(MPC)-grafted substrates based on a novel synthetic method of polymer composites and SI-ATRP. 3D modification was that phospholipid polymer were grafted from the surface of the polymer composite by SI-ATRP of MPC. By varying the [MPC]/[sacrificial initiator] ratio, a set of surfaces corresponding to various graft chain lengths was prepared. The density of the PC groups on the surface, which are closely related to the hydrophilicity, increased with the length of the grafted poly(MPC) chains. The surfaces with high poly(MPC) chain lengths showed a drastic reduction in protein adsorption. The surface with an arbitrary structure and the characteristic can be constructed by using 2D and 3D modification. In addition, another monomer enables to polymerize from the terminal halogen group of graft MPC polymer chain using SI-ATRP. The various functional bio-interface is constructed by the choice of next monomer with the functional groups such as carboxylic acid, amine, active ester, epoxy, and cell adhesion molecule. We conclude that the present process for preparing protein adsorption resistant surfaces on polymer composites by the SI-ATRP of MPC will provide an excellent method for developing new biomedical devices.

References

[1] Proteins at interfaces II, fundamentals and applications, T.A. Horbett, J.L. Brash (Eds.), ACS Symposium Series No. 602, ACS, Washington, DC, 1995.
[2] J.L. Brash, J. Biomater. Sci. Polym. Ed. 11 (2000) 1135.
[3] K. Ishihara, T. Ueda, N. Nakabayashi, Polym. J. 22 (1990) 355.
[4] T. Ueda, H. Oshida, K. Kurita, K. Ishihara, N. Nakabayashi, Polym. J. 24 (1992) 1259.
[5] K. Ishihara, R. Aragaki, T. Ueda, A. Watanabe, N. Nakabayashi, J. Biomed. Mater. Res. 24 (1990) 1069.
[6] K. Ishihara, N.P. Ziats, B.P. Tierney, N. Nakabayashi, J.M. Anderson, J. Biomed. Mater. Res. 25 (1991) 1397.
[7] K. Ishihara, H. Oshida, T. Ueda, Y. Endo, A. Watanabe, N. Nakabayashi, J. Biomed. Mater. Res. 26 (1992) 1543.
[8] K. Ishihara, H. Nomura, T. Mihara, K. Kurita, Y. Iwasaki, N. Nakabayashi, J. Biomed. Mater. Res. 39 (1998) 323.
[9] A. Yamasaki, Y. Imamura, K. Kurita, Y. Iwasaki, N. Nakabayashi, K. Ishihara, Colloid Surf. B: Biointerfaces 28 (2003) 53.
[10] S. Sawada, S. Sakaki, Y. Iwasaki, N. Nakabayashi, K. Ishihara, J. Biomed. Mater. Res. 64A (2003) 411.
[11] K. Ishihara, D. Nishiuchi, J. Watanabe, Y. Iwasaki, Biomaterials 25 (2004) 1115.
[12] N. Morimoto, A. Watanabe, Y. Iwasaki, K. Akiyoshi, K. Ishihara, Biomaterials 25 (2004) 5353.
[13] S.H. Ye, J. i Watanabe, K. Ishihara, J. Biomater. Sci. Polym. Ed. 15 (2004) 981.
[14] T. Moro, Y. Takatori, K. Ishihara, T. Konno, Y. Takigawa, T. Matsushita, U.I. Chung, K. Nakamura, H. Kawaguchi, Nat. Mater. 3 (2004) 829.
[15] T. Goda, T. Konno, M. Takai, T. Moro, K. Ishihara, Biomaterials 27 (2006) 5151.
[16] J.B. Kim, W.X. Huang, M.D. Miller, G. Baker, M.L. Bruening, Polym J. Sci. Part A: Polym. Chem. 41 (2003) 386.
[17] W. Feng, S. Zhu, K. Ishihara, J.L. Brash, Langmuir 21 (2005) 5980.
[18] W. Feng, S. Zhu, K. Ishihara, J.L. Brash, Biointerphases 1 (2006) 50.
[19] R. Iwata, P.S. In, V.P. Hoven, A. Takahara, K. Akiyoshi, Y. Iwasaki, Biomacromolecules 5 (2004) 2308.
[20] T. Hoshi, T. Swaguchi, T. Konno, M. Takai, K. Ishihara, Polymer 48 (2007) 1573.
[21] T. Hoshi, T. Swaguchi, R. Matsuno, T. Konno, M. Takai, K. Ishihara, J. Supercrit. Fluids 44 (2008) 391.
[22] K. Yamamoto, Y. Miwa, H. Tanaka, M. Sakaguchi, S. Shimada, J. Polym. Sci. A: Polym. Chem. 40 (2002) 3350.
[23] T. Teraya, A. Takahara, T. Kajiyama, Polymer 31 (1990) 1149.
[24] K. Ishihara, Sci. Technol. Adv. Mater. 1 (2000) 131.

Colloids and Surfaces B: Biointerfaces 67 (2008) 216–223

Contents lists available at ScienceDirect

Colloids and Surfaces B: Biointerfaces

journal homepage: www.elsevier.com/locate/colsurfb

Surface immobilization of biocompatible phospholipid polymer multilayered hydrogel on titanium alloy

Jiyeon Choi[a], Tomohiro Konno[a,c], Ryosuke Matsuno[a,c], Madoka Takai[a,c], Kazuhiko Ishihara[a,b,c,*]

[a] Department of Materials Engineering, School of Engineering, The University of Tokyo, 7-3-1, Hongo, Bunkyo-ku, Tokyo 113-8656, Japan
[b] Department of Bioengineering, School of Engineering, The University of Tokyo, 7-3-1, Hongo, Bunkyo-ku, Tokyo 113-8656, Japan
[c] Center for NanoBio Integration, The University of Tokyo, 7-3-1, Hongo, Bunkyo-ku, Tokyo 113-8656, Japan

ARTICLE INFO

Article history:
Received 21 May 2008
Received in revised form 19 August 2008
Accepted 21 August 2008
Available online 16 September 2008

Keywords:
Phospholipid polymer
Hydrogel
Multilayer
Titanium
Biocompatibility

ABSTRACT

The aim of this study is to improve the biocompatibility of titanium alloy (Ti) implants by immobilization of multilayered phospholipid polymer hydrogel able to reduce protein adsorption and cell adhesion. We fabricated and characterized a multilayered hydrogel on Ti substrate via a layer-by-layer self-assembly deposition method using a phospholipid polymer bearing a phenylboronic acid moiety and poly(vinyl alcohol) (PVA). The water-soluble phospholipid polymer (PMBV) was synthesized from 2-methacrylocyloxyethyl phosphorylcholine, *n*-butyl methacrylate, and 4-vinylphenylboronic acid (VPBA). The PMBV reacted with PVA and formed a hydrogel due to covalent linkage between the VPBA units and hydroxyl groups of PVA. The hydrogel layer growth on the Ti surface was initialized by the deposition of one layer of photoreactive PVA bonded by UV irradiation to the Ti surface, which was modified with an alkylsilane compound. The multilayered hydrogel was built up by alternating the deposition of the PMBV and PVA; this was monitored by several methods: static contact angle measurement, X-ray photoelectron spectroscopy, and attenuated Fourier-transform infrared spectroscopy. The results revealed clearly the progressive construction of the multilayered hydrogel on the Ti substrate. The PMBV/PVA multilayer prepared on the Ti substrate reduced the adhesion of L929 cells compared with that on an untreated Ti substrate. Thus, we concluded that the formation of the multilayered hydrogel is effective to improve the biocompatibility on Ti-based medical devices.

1. Introduction

When medical implants come into contact with the biological environment, various biological responses ranging from the adsorption of biomolecules to cell attachment and tissue response should occur [1]. The design of biomedical devices for controlling the physical, chemical and biochemical properties of an implant surface is important since the unfavorable interaction at the interface between an implant and biological environment might lead to implant failure, complications with high morbidity and treatment costs [2,3]. Among the various biomaterials used for load-bearing applications, such as orthopedic and cardiovascular implants, titanium and its alloys (Ti) is the key material owing to its excellent tissue compatibility and corrosion resistance that stems from the native oxide layer. This oxide layer sometimes is beneficial to the adsorption of many proteins for healing process. However, in blood-contacting devices, the bare Ti surface activates the intrinsic pathway of coagulation and promotes unnecessary protein adsorption due to the negative surface charge [4]. Therefore, the achievement of an implant surface which enhances the biocompatibility while inhibiting protein adsorption and cell adhesion for preventing undesirable responses towards implants in living systems can potentially have biomedical application.

Modifications of biomaterial surfaces have a long history in implantology and form a major area of research. Among the considerable number of biomaterials that have been developed thus far, the phospholipid polymers prepared from 2-methacryloyloxyethyl phosphorylcholine (MPC) and other vinyl compounds have shown the greatest promise; they mimic the natural cell membrane surface and are, therefore, inherently resistant to biofouling by proteins. Moreover, it is known as they perform better than most other types of polymeric materials with respect to their resistance to protein adsorption, cell adhesion, and whole blood coagulation. For these reasons, MPC polymers are currently being widely used in the biomedical field for surface modification [5–16].

Since its introduction by Decher in 1992 [17,18], the process of building up organic multilayer films through layer-by-layer self-assembly (LbL) has been attracted a great deal of attention and allows the formation of interpolymer complexes by the deposi-

* Corresponding author at: Department of Materials Engineering, The University of Tokyo, 7-3-1, Hongo, Bunkyo-ku, Tokyo 113-8656, Japan. Fax: +81 3 5841 8647.
E-mail address: ishihara@mpc.t.u-tokyo.ac.jp (K. Ishihara).

0927-7765/$ – see front matter © 2008 Elsevier B.V. All rights reserved.
doi:10.1016/j.colsurfb.2008.08.025

tion of oppositely charged polyelectrolytes. The LbL method is renowned for being a convenient, versatile, and efficient technique to generate biologically active surfaces. In addition, compared with conventional polymer coating, it affords more stable coating and various applications because of chemical bonding between layer to layer, such as controlled drug release [19], cell–surface interaction [20] and surface modification [21]. Furthermore, various driving forces have been introduced for forming multilayers by the LbL method, such as electrostatic interaction [22–24], hydrogen bonding [25–28], and covalent bonding [29].

This study employed covalent bonding-driven self-assembly to produce polymer hydrogel multilayers on Ti surfaces. We adopted a phospholipid polymer (PMBV) containing 2-methacryloyloxyethyl phosphorylcholine, *n*-butyl methacrylate (BMA), and 4-vinylphenylboronic acid unit (VPBA). The hydrophobic BMA unit can regulate the solubility of MPC polymer and also form the hydrophobic domain in aqueous condition, which dissolve hydrophobic bioactive agents, such as paclitaxel [11]. Phenylboronic acid in a tetrahedral anionic structure is known to rapidly form a cyclic boronic complex with cis-diols [30], for example, carbohydrates such as glucose, catechol derivatives such as dopamine, and some polymers such as poly(vinyl alcohol) (PVA) [31,32]. The interpolymer complexation of a polymer comprising boronic acid with PVA has been reported to form a hydrogel due to the covalent linkage in both constituent polymers and this hydrogel is reversibly dissociated by the addition of glucose [33–35].

We expected that the LbL deposition method would enable the combination of PMBV and PVA to produce a polymer hydrogel multilayer bonded to Ti. Therefore, the objective of this study was to fabricate and characterize Ti surfaces modified with PMBV and PVA via the LbL method for improving biocompatibility of Ti implant. By constructing a multilayered hydrogel on the Ti surface, the surface may become much more biocompatible, and moreover, the multilayered hydrogel layer can have a functional stage for the sustained release of biologically active molecules.

2. Experimental

2.1. Materials

MPC was obtained from NOF (Tokyo, Japan); it was synthesized using a method proposed by Ishihara et al. [5]. *n*-Butyl methacrylate was purchased from Nacalai Tesque Co. Ltd. (Tokyo, Japan). VPBA and PVA (degree of polymerization: 1500) were purchased from Wako Pure Chemical Industries, Ltd. (Osaka, Japan). Octadecyltriethoxysilane (ODS) were purchased from ShinEtsu Chemical Co. Ltd. (Tokyo, Japan). Photoreactive PVA (AWP, azide-unit pendented water-soluble PVA) was purchased from Toyo Gosei Co. Ltd., Japan. Titanium alloy (Ti) substrates were obtained from DENISPY-Sankin K.K. (Tokyo, Japan). The other reagents and solvents were of the extra-pure grade and were used without further purification.

2.2. Synthesis of PMBV

PMBV was synthesized by the conventional radical polymerization of the corresponding monomers: the desired amounts of MPC, BMA, and VPBA were dissolved in ethanol taken in an ampoule. The total concentration of monomer was adjusted to 1.0 mol/L. An initiator, α,α'-azobisbutyronitrile (AIBN), was added to the ampoule at a concentration of 1.0 mmol/L. Next, argon gas was bubbled into the solution for 10 min to eliminate oxygen and the ampoule was then sealed. Polymerization was carried out at 60 °C for 2.5 h. After cooling, the contents were poured into a large amount of diethylether and chloroform (8:2 by volume) to remove any unreacted monomers and to yield PMBV. The precipitant was collected and dried *in vacuo*. The structure of the copolymer was confirmed with ^{1}H-NMR (α-300, JEOL, Tokyo, Japan) and a Fourier-transform infrared spectrometer (FT-IR; FT/IR-615, JASCO, Tokyo, Japan). The molecular weight was determined by gel permeation chromatography (GPC, JASCO, Tokyo, Japan). The chemical structure of PMBV is shown in Fig. 2.

2.3. Fabrication of multiplayer

2.3.1. Preparation and cleaning of Ti

Two types of Ti substrates were used. The Ti substrates were prepared from a Ti plate (thickness: 0.5 mm) by cutting it into 10 mm × 10 mm square pieces.

These were rinsed in acetone and ethanol using sonification for 15 min each. After drying in air, the samples were oxidized as follows: They were immersed in a 3:1 (v/v) mixture of concentrated H_2SO_4 and 30% H_2O_2 for 1 h at 25 °C. The samples were then rinsed three times with distilled water and dried in an oven at 60 °C. To evaluate the thickness of the multilayered hydrogel, quartz substrates (10 mm × 15 mm × 0.8 mm; Matsunami, Tokyo, Japan) were coated with a 100-nm-thick Ti layer by RF magnetron sputtering (Ulvac Kiko, Inc., Tokyo, Japan, duration: 4 min, pressure: $\sim 2 \times 10^{-3}$ Pa). The quartz substrates were cleaned using an oxygen plasma apparatus (PR500 plasma reactor, Yamato Science, Tokyo, Japan) for 20 min. Finally the Ti-sputtered substrates were oxidized using the oxygen plasma apparatus for 10 s, and silanization was carried out immediately afterward.

2.3.2. Silanization on Ti substrate

A monolayer of ODS was prepared by the following procedure: First, 10 mM ODS was dissolved in anhydrous toluene. The Ti substrates were then immersed in the ODS solution and reacted for 24 h at 80 °C. And finally, the Ti substrates were rinsed in toluene three times and dried *in vacuo* at room temperature.

2.3.3. Fabrication of multilayer on Ti substrate

The ODS-treated Ti substrates were coated with an aqueous solution of AWP (1 wt%) by dip coating. The AWP-coated Ti substrates were air-dried under a fume hood at room temperature. After applying the AWP coating, the Ti substrates were irradiated with UV light (135 mW/cm^2) using a UV Spot Cure (SP-7, Ushio Inc., Yokohama, Japan) for 40 s.

PMBV solutions with concentrations of 50 and 25 mg/mL and PVA solutions with concentrations of 15 and 30 mg/mL were prepared with distilled water. The combinations of PMBV and PVA solutions examined are as follows: PMBV 50 mg/mL and PVA 15 mg/mL (PMBV50/PVA15), PMBV 25 mg/mL and PVA 30 mg/mL (PMBV25/PVA30), and PMBV 25 mg/mL and PVA 15 mg/mL (PMBV25/PVA15). The multilayer construction was accomplished by alternately dipping the Ti substrates with bonded AWP in the PMBV and PVA solutions for 10 min each and subsequently rinsing them with distilled water for 1 min. Six layers (3-bilayers) terminated with a layer of PMBV were obtained by the LbL method.

2.4. Characterization of multilayers

The thickness of the polymer multilayer was characterized by field emission scanning electron microscopy (FE-SEM, S-4200, Hitachi, Japan). Multilayers were built up as described above on the surface of the Ti-sputtered quartz substrates. And the cross-section of the quartz substrate was analyzed after the formation of each layer. Gravimetric measurements were performed after each successive layer was constructed. The swelling ratios of the multilayered hydrogel on the Ti surface were obtained at room

temperature. Multilayered hydrogels in triplicate were incubated in phosphate-buffered saline (pH 7.4) and their dry weights were measured beforehand. Then, the swelling ratios were calculated by the following equation:

$$\text{Swelling ratio}(\%) = \left[\frac{(W_s - W_d)}{W_d}\right] \times 100$$

where W_s and W_d are the weights of the swollen and dry hydrogel, respectively.

The static water contact angle on the prepared surfaces was measured using the sessile drop method at the ambient temperature using a contact angle goniometer (G-1, Erma, Tokyo, Japan). Images of water spreading on the sample surfaces were recorded by a camera and then analyzed using the software supplied by the manufacturer. Five measurements were made for each sample. For captive bubble method, the glass cell was filled with ultrapure water and 1 cm^2 samples of test solids were placed in it. A special L shaped syringe needle containing air releases bubbles beneath the sample. A computer screen provided an image of the captive bubble and then analyzed using the software supplied by the manufacturer. In addition, infrared spectral analysis was performed by attenuated Fourier-transform infrared spectroscopy (ATR-FTIR, IMV-4000, FT/IR-6300, JASCO, Tokyo, Japan). The spectra were examined visually, with special interest given to the spectral range of 4000–850 cm^{-1}.

For chemical composition analysis, specimens were characterized using X-ray photoelectron spectroscopy (XPS; AXIS-His165 Kratos/Shimadzu, Kyoto, Japan) with a focused monochromatic Mg Kα X-ray source (1253.6 eV) for excitation. The electron take-off angle was 60° in the dry state and the analyzer was operated in the constant energy mode for all measurements.

2.5. Cell culture and cell morphology

For cell adhesion, L929 cells were cultured in a culture medium (D-MEM (Gibco), supplemented with 10% (v/v) fetal calf serum (FBS)) at 37 °C in an atmosphere of 5% CO_2 at 95% humidity. The cells were seeded at a density of 4×10^4 cells/mL on the experimental substrates and were cultured for 1 day. Subsequently, cell fixation was carried out for 90 min in 2.5% glutaraldehyde solution at 4 °C. Then, the samples were washed twice with PBS and dehydrated using a graded series of ethanol solutions (70%, 90%, and 100%) for 15 min each and were subsequently dried with 1,1,1,3,3,3-hexamethyldisilane. The morphology of the adherent cells was observed using a scanning electron microscope (SEM, SM-200, Topcon, Tokyo, Japan) after depositing gold.

3. Results

3.1. Characterization of PMBV

The copolymerization of MPC, BMA, and VPBA proceeded well and a polymer containing these monomer units was obtained; the obtained PMBV was water-soluble. The spectral data from ^{1}H-NMR and FT-IR revealed the chemical structure of the obtained PMBV.

Fig. 1 shows a schematic illustration of the process for fabricating the multilayered hydrogels on the Ti substrates via the LbL method (a) and the mechanism of PMBV/PVA hydrogel formation (b). The chemical structure and synthetic results of the obtained PMBV are summarized in Fig. 2 and Table 1.

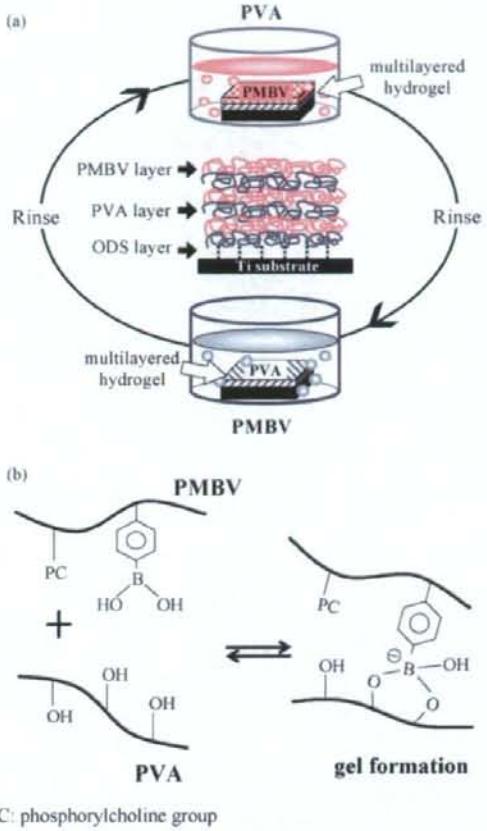

Fig. 1. (a) Schematic representation of construction procedure for the multilayered hydrogels on the Ti substrates. (b) Reaction between the phenylboronic acid moiety in PMBV in an aqueous solution and a polyol moiety in the presence of PVA.

3.2. Multilayered hydrogel formation from PMBV/PVA system

The preparation of the PMBV/PVA hydrogel layers on the Ti substrates via the LbL method was followed by a change in the weight

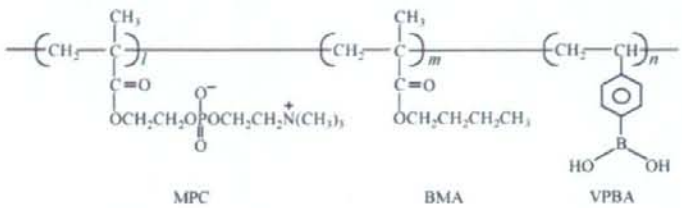

Fig. 2. Chemical structure of PMBV.

Table 1
Synthetic result of PMBV.

Abb	Monomer unit composition (mol%)[a]		Yield(%)	Molecular weight Mw($\times 10^4$)[b]
	In feed MPC/BMA/VPBA	In polymer MPC/BMA/VPBA		
PMBV	60/30/10	57/25/18	70	6.5

$[Monomer]_{total}$ = 1.0 mol/L in EtOH; [AIBN]=1 mmol/L; copolymerization time: 2.5 h, polymerization temperature 60 °C.
[a] Determined by ^{1}H-NMR.
[b] Determined by GPC.

Table 2
Characterization of polymer multilayer.

Polymer concentration (mg/mL) [PMBV]/[PVA]	Cumulative weight increase (mg) ± SD			Swelling ratio ± SD (%)
	Number of layer			
	2	4	6	
50/15	0.19 ± 0.01	0.96 ± 0.10	1.98 ± 0.23	440 ± 70
25/15	0.20 ± 0.14	0.31 ± 0.23	0.74 ± 0.42	340 ± 50

of the substrates; the results are shown in Table 2. Weight measurements showed an increase in the multilayered hydrogel on the Ti surface as a function of even numbers of coating layers. The cumulative weights of PMBV50/PVA15 and PMBV25/PVA15 after the formation of the 3-bilayer were measured as 1.98 ± 0.23 and 0.74 ± 0.42 mg, respectively. Moreover, the swelling ratios of the 3-bilayer hydrogels from the dried state in an aqueous medium were estimated by the weight change after allowing equilibration for 1 day; the results are shown in Table 2. PMBV50/PVA15 exhibited a higher swelling ratio than PMBV25/PVA15; the former exhibited a swelling ratio of 440 ± 70% and the latter, 340 ± 50%. The ATR-FTIR spectrum of each outer layer formed during the fabrication process is shown in Fig. 3. As the specific surfaces changed gradually from Ti to PMBV, each spectrum expressed the particular peaks associated with the functional groups of that surface. After the bare Ti surface (Fig. 3(a)) treated the silanization, the ODS-treated Ti surface (Fig. 3(b)) exhibited the band corresponding to ≡Ti–O–Si≡ in the region of 970–1000 cm^{-1}. And

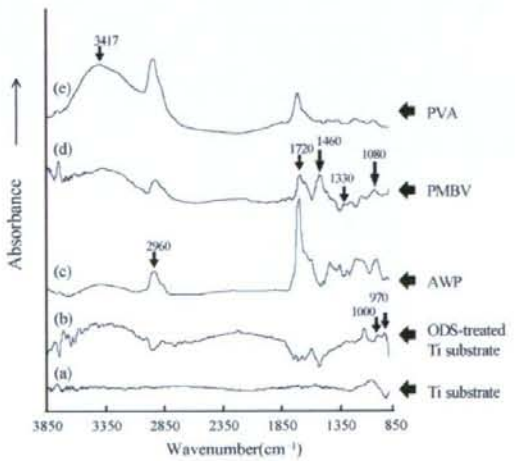

Fig. 3. ATR-FTIR spectra of (a) Ti substrate, (b) ODS-treated Ti substrate, (c) AWP, (d) PMBV, and (e) PVA. In this case, the multilayered hydrogel of PMBV25/PVA30 was used.

after bonding the AWP layer (Fig. 3(c)) to the ODS-treated Ti surface, the spectrum exhibited characteristic vibration at 1720 cm^{-1} for the carbonyl group, and at 1650 and 1463 cm^{-1} for the C=C of aromatic ring. However, no azide peak was observed around 2200 cm^{-1}. After complexation with PMBV (Fig. 3(d)), the phosphate group in the MPC unit could be seen at 1080 and 970 cm^{-1}, and peaks at 1720 and 1460 cm^{-1} corresponding to C=O carbonyl stretching and $-CH_2-$ bending were also observed, respectively. The appearance of peaks at 1330 and 1350 cm^{-1} is attributed to the B–O stretching modes in phenylboronic acid. In Fig. 3(e), the peak around 3417 cm^{-1} is associated with the –OH bands in PVA. The thickness of the PMBV/PVA hydrogel increased as a function of the number n of deposited layers (Fig. 4). The final thicknesses of PMBV50/PVA15, PMBV25/PVA30, and PMBV25/PVA15 were determined as 8, 7, and 6 μm by SEM measurements of the cross-sections of the hydrogel layers on the Ti-sputtered quartz, respectively.

3.3. Surface property of the multilayered hydrogel

The contact angle depends on the character of surface wettability, and measurements were performed to confirm the alternate deposition of PMBV and PVA. Polymer hydrogel layers made by layer-by-layer methods on Ti surfaces are expected to alternately change surface wettability. Fig. 5 shows the results of the static water contact angle by sessile drop method and by the captive bubble method for three polymer combinations. In case of the sessile drop method (Fig. 5(a)), the static water contact angle for PVA 15 and 30 mg/mL is approximately 60°, and that for PMBV 25 and 50 mg/mL is 80°. The subsequent adsorption of PMBV made the surface slightly hydrophobic compared to that with the PVA surface in dry condition. However, in the case of captive bubble method (Fig. 5(b)), while PVA layers are approximately 40°, most of PMBV layers are 20° and all of the 6th layers are 0° regardless of PMBV concentrations. This means the outmost layers of multilayered hydrogel are totally covered with PMBV. The alternation of the static contact angle and captive bubble contact angle strongly indicates that the hydrogel layers were constructed regularly. XPS is useful tool for obtaining qualitative and quantitative information of the different elements at a substrate surface. XPS was used to monitor each deposition step as it can provide information on the surface phosphorus/carbon ratio (P/C ratio) on the Ti samples coated with different deposition layers; the results are

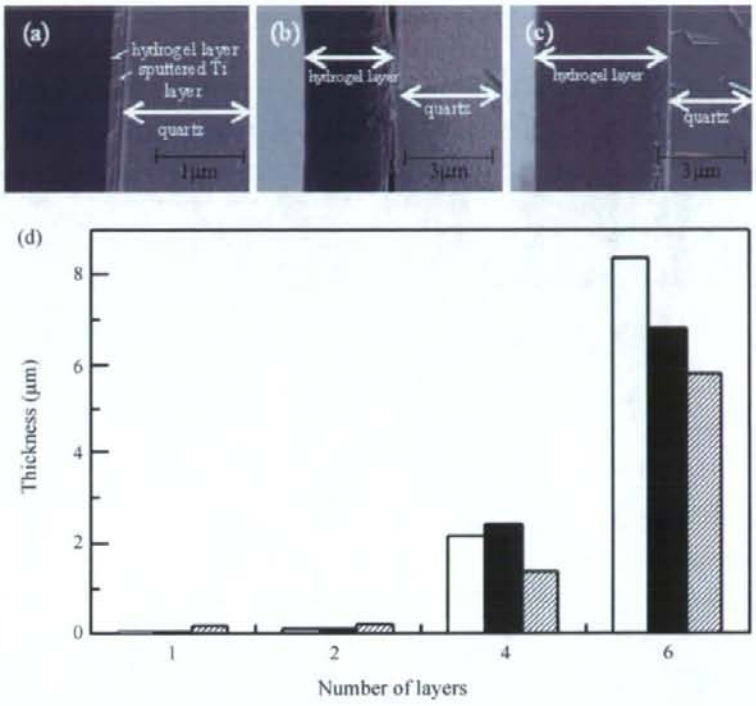

Fig. 4. Cross-sectional SEM images of multilayered hydrogel with (a) second layer (b) fourth layer, and (c) sixth layer of PMBV25/PVA30. (d) Hydrogel layer thickness of PMBV/PVA measured by SEM as a function of layer number. In this case, samples with an even number of layers have PMBV, whereas samples with an odd number of layers have PVA: (□) PMBV50/PVA15, (■) PMBV25/PVA30, and (▨) PMBV25/PVA15. Multilayered hydrogels were constructed on Ti-sputtered quartz substrates. The results are the means of the results of three independent experiments.

presented in Fig. 6. As the deposition cycle was repeated, P/C ratio could discriminate the presence or absence of a PMBV layer; that is, PMBV-terminated layers (the even number) exhibited 4 times larger P/C values.

3.4. Cell adhesion on the multilayered hydrogel

The morphological aspects of L929 cells grown on the differently loaded multilayered hydrogel coatings were evaluated using an SEM (Fig. 7). On a plain Ti substrate (Fig. 7(a,b)) and on one modified with AWP (Fig. 7(c,d)), the adhesion and proliferation of L929 cells was observed during a 1-day culture, as usual. However, apparent differences in cell morphology were found on PMBV (Fig. 7(e,f)) and PVA (Fig. 7(g,h)) as compared to that on the Ti substrate and AWP-modified substrate. That is, the number of L929 cells that adhered to the PMBV and PVA surfaces was significantly lesser than those on the Ti substrate and photoreactive PVA. In addition, the L929 cells did not preserve their normal spindlelike shape, but exhibited circular, round shapes.

4. Discussion

This study focused on the fabrication and characterization of multilayered hydrogels using water-soluble MPC polymers bearing a phenylboronic acid moiety and PVA via the LbL deposition method. Phenylboronic acid is one of the most familiar reactive groups used to synthesize stable covalent complexes with polyol compounds, including PVA. Because of the strong binding, it can be used as a recognition moiety in sugar fractionation. However, besides sugar recognition, the usage of polyols such as PVA has permitted the present system to form hydrogels without any chemical crosslinking treatment. Moreover, the use of PVA in hydrogels has attracted considerable attention because of its inherent low toxicity and high degree of swelling in water [33]. The LbL method is a desirable and versatile tool for assembling PMBV and PVA into a multilayered hydrogel. In this study, we have chosen the concentration of polymer capable of forming hydrogel upon mixing aqueous solutions in physiological condition, whose conditions depend on the concentrations of PMBV and PVA. The gelation did not affect the ionic strength [34]. After constructing multilayered hydrogel, we observed the chemical bonding between layer to layer through unique peaks of FT-IR. However, it was not clear to confirm the bonding between phenylboronic acid and polyol because the change of peak corresponding to –B–O stretching appeared from 1330 to 1350 cm^{-1}.

Based on the increases in both the weight and thickness of the substrates, we confirmed that the LbL method was feasible with the PMBV/PVA system. The build-up of multilayered films arises from covalent bonding between alternately deposited PMBV and PVA. In case of thickness, the concentration of AWP coated on Ti substrate was lower than that of PMBV and PVA constructing multilayer by LbL method, that is, the number of binding sites are different. This is why the difference of thickness between 1st layer and 2nd layer

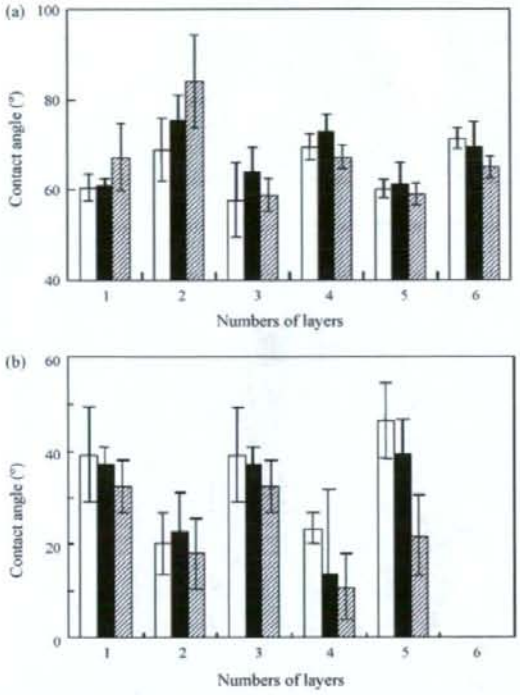

Fig. 5. The static water contact angles (a) by sessile drop method and (b) by captive bubble method on the PMBV/PVA multilayered hydrogel surface as a function of the layer number. In these cases, samples with an even number of layers have PMBV, whereas samples with an odd number of layers have PVA: (□) PMBV50/PVA15, (■) PMBV25/PVA30, and (▨) PMBV25/PVA15. The results are expressed as the mean ± SD for three independent experiments.

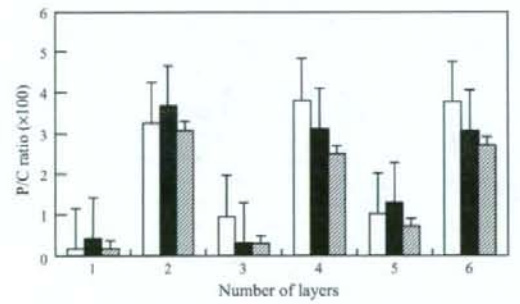

Fig. 6. P/C ratio of multilayered PMBV/PVA hydrogel layer. The even numbers correspond to PMBV as the outmost layer and the odd numbers correspond to PVA as the outmost layer: (□) PMBV50/PVA15, (■) PMBV25/PVA30, and (▨) PMBV25/PVA15. The results are expressed as the mean ± SD for three independent experiments.

cannot observe. From 2nd layer to 6th layer, the thicknesses have increased linearly and have been influenced in the concentration of polymers. The number of cycles and the concentrations of polymer solution modulate the thickness [24,35]. The change in both weight and thickness of the hydrogel layer depend on the polymer concentrations. PMBV/PVA multilayered hydrogel appeared high swelling ratio without regard for polymer concentration. It means both of PVA and PMBV containing hydrophilic PC-group are familiar to water molecules. It is thought that the contact angle data also support hydrophilic property of these polymers. Both of the contact angle measurement revealed that the outmost layer was exchanged alternatively. In particular, as the captive bubble method indicates the wettability of surface in wet condition, we could obtain interesting information by comparing the results of the sessile drop method. When the outermost layer was PMBV, the contact angle in dry condition increased over that with PVA. This means the surface of PMBV layer is covered with hydrophobic group, that is, phenylboronic acid and butyl group of BMA. However, the contact angle of PMBV in wet condition is dramatically opposed to that in dry condition. It is due to the rapid adsorption of the water molecules around the hydrophilic PC-groups in the PMBV [36]. In all of case, the contact angle of 6th layer is zero (Fig. 5(b)). It is thought that the outmost surfaces are covered with PMBV. On the other hand, PVA layers keep similar surfaces covered with hydroxyl groups regardless of whether it is in dry condition or it is in wet condition. From both of contact angle data, although it is known that PC-containing polymer, PMBV, and PVA are hydrophilic, we could observe the change of surface property in dry and wet condition. According to the change of layer surface from PVA to PMBV, the P/C ratio in XPS increased because of the influence of PMBV, which contains a phosphorylcholine group. The measurements of the static contact angle and the XPS results are susceptible to the surface property. In addition, the ATR-FTIR data showed that the Ti substrates were connected to the organic polymer material by silanization and photoreaction with AWP. Although the infrared spectral criterions of the azide structure have a characteristic around 2200–2300 cm^{-1}, it was thought that no trace was observed because ODS and AWP were bonded together by UV irradiation.

The cellular behavior is an important factor for interpreting the biocompatibility of biomaterial. The cell morphology images revealed that Ti and AWP surfaces permitted the adhesion, spreading, and migration of L929 cells to degrees that PVA and PMBV surfaces did not. The adhesion of cells to surfaces is dependant on the adsorption of highly adhesive proteins such as fibronetin and vitronectin, which link cells to the biomaterial surface. Cell–substrate interaction is mainly based on the recognition of Arg-Gly-Asp (RGD) sequences by receptors located on the cell surface. As AWP allows easy immobilization of specific proteins, it has been studied for application to microarray chips and cell adhesion assays [37]. It is generally accepted that hydrophilic polymers such as poly(ethylene oxide)-based polymers and phosphorylcholine-functioned polymers do not allow protein adsorption at their surface. Thus, they can reduce the adhesion of cells, including fibroblasts, platelets, and macrophages [9,10,38]. A wide variety of polymers containing charges, including anionic DNA and cationic chitosan, have been used for the construction of multilayerd coatings with the aim to modulate cell behavior. In particular, various studies with cells, including fibroblast and osteoblast, have shown that polyelectrolyte multilayered coatings are useful tool to regulate biomaterial surface through in vitro experiment of cell proliferation and viability [21,39]. In this study, the MPC polymer-hybridized Ti substrates and multilayered hydrogels offer the potential for preparing blood-contacting materials via the incorporation of the outmost layer, PMBV, which inhibits the adsorption of proteins and the adhesion of cells. Moreover, we note that bioactive reagents may be incorporated in the multilayered hydrogel to allow for sustained release using hydrophobic domain of BMA unit. Hence, the release behavior of a bioactive reagent from a Ti substrate with an immobilized hydrogel is currently under investigation in the laboratory and the results will be reported in the near future.

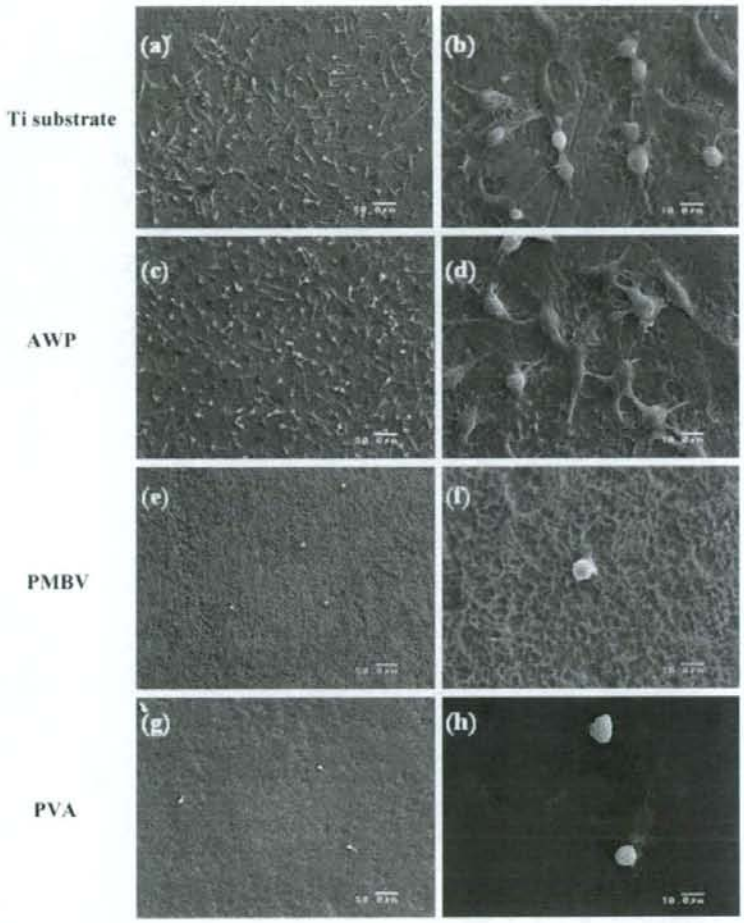

Fig. 7. SEM images of L929 cell morphology adhered on a Ti substrate (a, b) and on Ti substrates modified with AWP (c, d), PMBV (e, f), and PVA (g, h) after a 1-day culture. The PMBV and PVA concentration were 25 and 30 mg/mL, respectively.

5. Conclusions

This study demonstrates the feasibility of the LbL method in constructing multilayered hydrogels composed of the PMBV/PVA system on Ti substrates for improving biocompatibility of implant surface. The basic mechanism for the construction of the multilayered hydrogels was the selective reactions between the boronic acid moiety in PMBV and the hydroxyl groups in PVA. To initiate the LbL process, a silane coupling reaction was used to introduce an alkyl group on the Ti substrates, and AWP could bind covalently to the substrate surface by photoirradiation. Subsequently, the PMBV/PVA hydrogel system was fabricated. The process was followed by contact angle measurements and XPS analyses; these results indicated that the surface properties changed alternatively, reflecting the nature of the polymer on the outer surface. The thickness of the hydrogel increased with the number of layers. These data suggested that PMBV/PVA successfully covered the Ti substrate surface. Furthermore, PMBV, the outmost layer, was found to inhibit cell attachment. Moreover, the hydrogel layer can effectively entrap bioactive reagents and control their diffusivity. Research on this is currently underway in our laboratory and the results will be reported in the near future.

We concluded that the Ti substrates with multilayered polymer hydrogels will be useful in applications such as implantable devices and local drug delivery systems.

Acknowledgment

This study was partially supported by the Mitsubishi Foundation (Research grants in the natural sciences) in 2007.

References

[1] B. Kasemo, Surf. Sci. 500 (2002) 656.
[2] S. Tosatti, S.M. De Paul, A. Askendal, S. VandeVondele, J.A. Hubbell, P. Tengvall, M. Textor, Biomaterials 24 (2003) 4949.
[3] P.H. Chuna, K.G. Neoh, E.T. Kang, W. Wilson, Biomaterials 29 (2008) 1412.
[4] X. Liu, P.K. Chub, C. Dinga, Mater. Sci. Eng., R 47 (2004) 49.
[5] K. Ishihara, T. Ueda, N. Nakabayashi, Polym. J. 22 (1990) 355.
[6] T. Ueda, H. Oshida, K. Kurita, K. Ishihara, N. Nakabayashi, Polym. J. 24 (1992) 1259.

[7] K. Ishihara, N.P. Ziats, B.P. Tierney, N. Nakabayashi, J.M. Anderson, J. Biomed. Mater. Res. 25 (1991) 1397.
[8] K. Ishihara, H. Oshida, Y. Endo, T. Ueda, A. Watanabe, N. Nakabayashi, J. Biomed. Mater. Res. 26 (1992) 1543.
[9] K. Ishihara, H. Nomura, T. Mihara, K. Kurita, Y. Iwasaki, N. Nakabayashi, J. Biomed. Mater. Res. 39 (1998) 323.
[10] Y. Iwasaki, A. Mikami, N. Yui, K. Ishihara, N. Nakabayashi, J. Biomed. Mater. Res. 36 (1997) 508.
[11] T. Konno, J. Watanabe, K. Ishihara, J. Biomed. Mater. Res. 65A (2003) 209.
[12] T. Moro, Y. Takatori, K. Ishihara, T. Konno, Y. Takigawa, T. Matushita, U.I. Chung, K. Nakamura, H. Kawaguchi, Nat. Mater. 3 (2004) 829.
[13] J. Sibarani, M. Takai, K. Ishihara, Colloid Surf. B 54 (2007) 88.
[14] Y. Xu, M. Takai, T. Konno, K. Ishihara, Lab Chip 7 (2007) 199.
[15] K. Nishizawa, T. Konno, M. Takai, K. Ishihara, Biomacromolecules 9 (2008) 403.
[16] J.H. Seo, R. Matsuno, T. Konno, M. Takai, K. Ishihara, Biomaterials 29 (2008) 1367.
[17] G. Decher, J.D. Hong, J. Shimit, Thin Solid Films 210 (1992) 831.
[18] G. Decher, Science 277 (1997) 1232.
[19] M.C. Berg, L. Zhai, R.E. Cohen, M.F. Rubner, Biomacromolecules 7 (2006) 357.
[20] T. Serizawa, M. Yamaguchi, T. Matsuyama, M. Akashi, Biomacromolecules 1 (2000) 306.
[21] K. Cai, A. Rechtenbach, J. Hao, J. Bossert, K.D. Jandt, Biomaterials 26 (2005) 5960.
[22] F. Caruso, K. Niikura, N.D. Furlong, Y. Okahata, Langmuir 16 (2000) 1249.
[23] S.S. Shiratori, M.F. Rubner, Macromolecules 33 (2000) 4213.
[24] K. Ren, J. Ji, J. Shen, Biomaterials 27 (2006) 1152.
[25] W.B. Stockton, M.F. Rubner, Macromolecules 30 (1997) 2717.
[26] J.F. Quinn, F. Caruso, Adv. Funct. Mater. 16 (2006) 1179.
[27] S.A. Sukhishvili, S. Granick, Macromolecules 35 (2002) 301.
[28] E. Brynda, M. Houska, J. Colloid Interface Sci. 183 (1996) 18.
[29] J. Yan, G. Springsteen, S. Deeter, B. Wang, Tetrahedron 60 (2004) 11205.
[30] Y. Ma, L. Qian, H. Huang, X. Yang, J. Colloid Interface Sci. 295 (2006) 583.
[31] A. Matsumoto, S. Ikeda, A. Harada, K. Kataoka, Biomacromolecules 4 (2003) 1410.
[32] S. Kitano, I. Hisamitsu, Y. Koyama, K. Kataoka, T. Okano, Y. Sakurai, Polym. Adv. Technol. 2 (1991) 261.
[33] P.R. Hari, K. Sreenivasan, J. Appl. Polym. Sci. 82 (2001) 143.
[34] T. Konno, K. Ishihara, Biomaterials 28 (2007) 1770.
[35] G. Ladam, P. Schaad, J.C. Voegel, P. Schaaf, G. Decher, F. Cuisinier, Langmuir 16 (2000) 1249.
[36] T. Goda, T. Konno, M. Takai, K. Ishihara, Colloids Surf. B: Biointerfaces 54 (2007) 67.
[37] Y. Ito, M. Nogawa, M. Takeda, T. Shinuya, Biomaterials 26 (2005) 211.
[38] K. Smetana Jr., Biomaterials 14 (1993) 1046.
[39] J.J.J.P. van den Beucken, X.F. Walboomers, M.R.J.N. Vos, A.J.M. Sommerdijk, R.J.M. Nolte, J.A. Jansen, J. Biomed. Mater. Res. 77A (2006) 202.

Polymer 49 (2008) 4652–4657

Contents lists available at ScienceDirect

Polymer

journal homepage: www.elsevier.com/locate/polymer

Hydration of phosphorylcholine groups attached to highly swollen polymer hydrogels studied by thermal analysis

Toshinori Morisaku [a], Junji Watanabe [b], Tomohiro Konno [a], Madoka Takai [a], Kazuhiko Ishihara [a,*]

[a] Department of Materials Engineering, School of Engineering and Center for NanoBio Integration, The University of Tokyo, 7-3-1 Hongo, Bunkyo-ku, Tokyo 113-8656, Japan
[b] Department of Applied Chemistry, Graduate School of Engineering, Osaka University, 2-1 Yamada-oka, Suita, Osaka 565-0871, Japan

ARTICLE INFO

Article history:
Received 14 February 2008
Received in revised form 2 August 2008
Accepted 15 August 2008
Available online 19 August 2008

Keywords:
2-Methacryloyloxyethyl phosphorylcholine polymer
Hydrogel
Nonfreezable water

ABSTRACT

Hydration of polymer chains plays a key role for determining the extent of protein adsorption on polymeric materials. Here we investigated the hydration of poly(2-methacryloyloxyethyl phosphorylcholine (MPC)) chains, which resist protein adsorption and following cell adhesion effectively. The hydration was compared with that of poly(methoxy oligo(ethylene glycol)-monomethacrylate ($Me(EG)_nMA$)) chains, which also have hydrophilic units. The poly(MPC) and poly($Me(EG)_nMA$) hydrogels with equilibrium water contents (EWCs) in the range from 86 to 97 wt% were prepared. By differential scanning calorimetric measurements, water in both the hydrogels was classified into two states: freezable and nonfreezable water. The poly(MPC) hydrogels had larger nonfreezable water than the poly($Me(EG)_nMA$) hydrogels even when their EWCs were similar, which indicated the higher hydrating ability of poly(MPC) chains. We suggested that the difference in the amount of nonfreezable water around polymer chains may influence the degree of protein adsorption resistance after contact with body fluid for a long period.

1. Introduction

According to the rapid advancement in developments of artificial organs, drug delivery systems, biochip-based diagnosis systems, and tissue engineering devices, the importance in the design of material surfaces that resist protein adsorption has been stressed [1–4]. Protein adsorption on material surfaces is the first phenomenon in contact with blood or tissues [5]. The adsorbed proteins are denatured, which is followed by platelet adhesions and cell adhesions for inducing thrombus formation and unfavorable immunoreactions. Thus, protein adsorption-resistant surfaces are essentially needed to obtain safe and stable medical treatment and diagnosis. Especially, cell-based tissue engineered devices and implantable artificial organs should have protein adsorption resistance surface for controlling cell/materials interactions for long period. To date, many protein adsorption-resistant surfaces have been designed. Recently, some research groups have achieved very low protein adsorption levels of $<10\ ng/cm^2$ by controlling the packing density and/or lengths of surface-tethered hydrophilic polymer chains [6–8]. On the other hand, the physico-chemical factors that determine the ability of the surfaces to resist protein adsorption have not been elucidated yet. A satisfactory understanding of such factors allows not only the systematic design of protein adsorption-resistant surfaces but also the elucidation of the mechanism of protein adsorption resistance.

Surface free energy on polymer materials has often been considered to be a key determinant of the extent of protein adsorption [9,10]. However, it has been demonstrated that there is no clear correlation between surface free energy and adsorbed amount of protein [11]. In addition, although the high conformational flexibility of surface-tethered chains has been experimentally and theoretically explained to make sterical inhibition of the access of proteins to surfaces by an excluded volume effect [12,13], it is not an essential requirement for protein adsorption resistance. In fact, self-assembled monolayers (SAMs) with polar functional end groups, such as short-chain poly(ethylene glycol) (PEG), i.e. oligo(ethylene glycol) (OEG), and an equimolar mixture of $-SO_3^-$ and $-N^+(CH_3)_3$ end groups, showed high resistance to protein adsorption [14,15].

The present discussion on the factors that determine the outcome of protein adsorption resistance is centered on the relationship between the hydration structures of material surfaces and protein adsorption [11,16]. The hydration structures of PEG chains have been intensively studied [17–19] because their utilization as surface modifiers is a well-known approach for rendering surfaces highly resistant to protein adsorption [6,9,11,14]. We have developed our original biocompatible polymer, poly(2-methacryloyloxyethyl phosphorylcholine) (poly(MPC)), which is inspired from the

* Corresponding author. Tel.: +81 3 5841 7124; fax: +81 3 5841 8647.
E-mail address: ishihara@mpc.t.u-tokyo.ac.jp (K. Ishihara).

0032-3861/$ – see front matter © 2008 Elsevier Ltd. All rights reserved.
doi:10.1016/j.polymer.2008.08.025

structure of phosphatidylcholines in cell membrane [4,20–22]. As a criterion of the hydration structures that provide the resistance of protein adsorption, the hydration structures of poly(MPC) chains provide us strong interest for understanding the biocompatibility. The surfaces grafted with the poly(MPC) chains resist platelet adhesion for longer periods than OEG-monomethacrylate polymer surfaces [23]. In addition, no conformation of albumin in poly(MPC) aqueous solutions changes during 72 h incubation, whereas albumin denatured by incubation in PEG aqueous solutions within 24 h [24]. Thus, it can be expected that the hydration of poly(MPC) chains may be different from that of PEG chains.

In this study, we investigated the hydration structures of poly(MPC) chains using a chemically cross-linked poly(MPC) hydrogel. The poly(MPC) hydrogels with six different equilibrium water contents (EWCs) were prepared in the range from 86.1 to 96.5 wt%. The different states of water absorbed in the hydrogels were classified and quantified by differential scanning calorimetry (DSC). They were compared with those in chemically cross-linked hydrogels composed of OEG-monomethacrylate polymer chains–poly(ω-methoxy tetra- or octa(ethylene glycol) monomethacrylate ($Me(EG)_nMA$) ($n = 4$ or 8)) chains– with a similar EWC range. The origin of nonfreezable water around poly(MPC) chains was also discussed.

2. Experimental section

2.1. Materials

The detailed synthetic process of MPC (Fig. 1a) has been reported elsewhere [20]. $Me(EG)_nMA$ (Fig. 1b) with molecular weights of 286 ($n = 4$) and 469 ($n = 8$) was purchased from Sigma–Aldrich (St. Louis, MO) and used without further purification. Ammonium peroxodisulfate (APS) (>98.0%, Kanto Chemicals, Tokyo, Japan), triethylene glycol dimethacrylate (TEGDMA) (>95%, Tokyo Kasei Kogyo, Tokyo, Japan), and *N,N,N′,N′*-tetramethylethylenediamine (TMEDA) (>98.0%, Kanto Chemicals) were also used without further purification. Distilled water was used for all sample preparations.

2.2. Preparation of chemically cross-linked poly(MPC) and poly($Me(EG)_nMA$) hydrogels

The procedure for preparing chemically cross-linked poly(MPC) hydrogels has already been described [25]. The poly($Me(EG)_4MA$) and poly($Me(EG)_8MA$) hydrogels were prepared by the same procedure. In brief, the hydrogels were prepared in an aqueous medium by free radical polymerization. An aqueous monomer solution, TEGDMA (1.0 mol% to a monomer) as a cross-linker, and a 0.22 mol/L APS aqueous solution (0.53 mol% to a monomer) as an initiator were placed in a Petri dish. The concentrations of the monomer solutions were 1.5, 1.75, 2.0, 2.25, 2.5, and 3.0 mol/L for MPC and 0.75, 1.0, 1.25, and 1.5 mol/L for $Me(EG)_4MA$ and $Me(EG)_8MA$. The solution in the Petri dish was stirred for 30 min to allow complete mixing. The solution began to make gelation 1 min after the injection of TMEDA (5.3 mol% to a monomer) as a catalyst. After its complete gelation, the obtained hydrogel was removed from the Petri dish, and subsequently, it was immersed in excess distilled water for 48 h to remove any unreacted compounds and to allow complete swelling. The water in the dish was replaced several times. All the fully swollen hydrogels were transparent. All these processes were carried out at room temperature. The fully swollen hydrogels were used for the following EWC and DSC measurements.

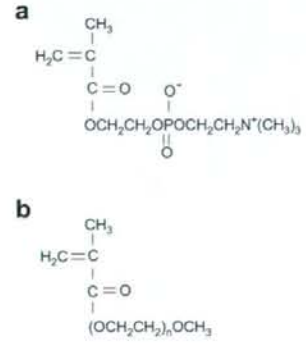

Fig. 1. Chemical structures of (a) MPC and (b) $Me(EG)_nMA$.

2.3. Determination of EWC

Each fully swollen hydrogel was freeze-dried for 24 h to remove the absorbed water. The weight of the freeze-dried hydrogel was recorded as W_d. The freeze-dried hydrogel was fully swollen again for 48 h. The excess water on the surface of the swollen hydrogel was gently removed with a filter paper before the measurement of its weight, W_s. The EWC of the hydrogel can be calculated by using the following equation.

$$\mathrm{EWC} = \frac{W_s - W_d}{W_s} \times 100 \quad (1)$$

2.4. DSC measurements

A 4–6 mg hydrogel was placed in an aluminum pan after gently wiping off the excess water on its surface, and then the pan was hermetically sealed. An empty aluminum pan was used as the control. Measurements were performed using an SII NanoTechnology (Chiba, Japan) model DSC6100 differential scanning calorimeter interfaced to an EXSTAR 6000 thermal analysis system version 5.8 (SII NanoTechnology). During the cooling and heating experiments, the sample cell was purged with nitrogen gas at a flow rate of 50 mL/min. The melting point peak of indium calibrated the temperature and heat flow of the equipment. The samples were initially cooled from room temperature to −70 °C at a rate of 5 °C/min and then heated to 40 °C at the same rate.

3. Results and discussion

Since the concentrations of water and polymer chains strongly influence their hydration properties, the poly(MPC) hydrogels with different EWCs were prepared. As shown in Fig. 2, the EWC of the poly(MPC) hydrogels could be controlled within the range of 86.1–96.5 wt%. To understand the effect of chemical structures on hydration, poly($Me(EG)_4MA$) and poly($Me(EG)_8MA$) hydrogels with a similar EWC range were prepared. The EWC of the poly($Me(EG)_4MA$) hydrogels and poly($Me(EG)_8MA$) hydrogels ranged from 87.5 to 95.9 wt% and 89.7 to 95.7 wt%, respectively. In the case of the poly($Me(EG)_8MA$) hydrogels, the EWC could not control below 89 wt% even when monomer solutions with concentrations higher than 1.5 mol/L were used.

Figs. 3–5 show the typical DSC heating thermograms of the poly(MPC), poly($Me(EG)_4MA$), and poly($Me(EG)_8MA$) hydrogels swollen with different EWCs, respectively. For comparison, the thermogram of bulk water is also presented in the respective figures. In the poly(MPC) hydrogels, a single endothermic peak was observed, and the transition occurred over a temperature range similar to that of the ice-to-water transition for bulk water. We

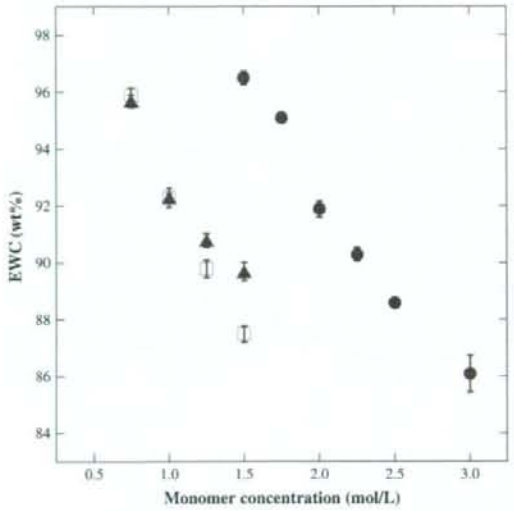

Fig. 2. EWC of the three types of hydrogels at the concentrations of the monomer solutions: poly(MPC) (●), poly(Me(EG)$_4$MA) (□), and poly(Me(EG)$_8$MA) (▲) hydrogels. The plotted values are the average of six measurements, and double the standard deviation is used as the range of errors in the values.

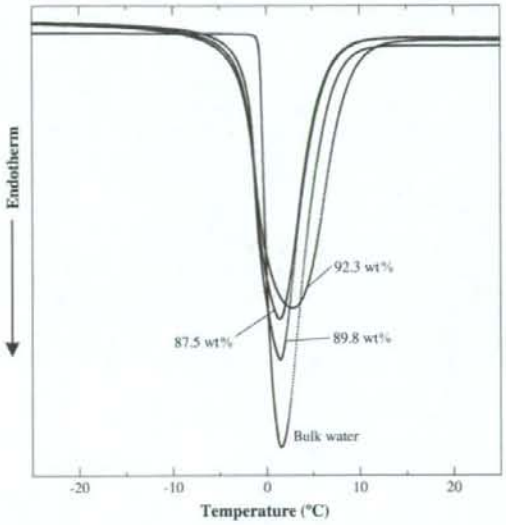

Fig. 4. DSC thermograms at a heating rate of 5 °C/min for the poly(Me(EG)$_4$MA) hydrogels with different EWCs and for bulk water. The values indicated in the figure show the EWCs.

could not observe any enthalpy change for freeze-dried poly(MPC) hydrogels in the temperature range, indicating that the polymer chains have no contribution to the endothermic behavior. Herein, it was concluded that the peak was derived from the melting of freezable water in the poly(MPC) hydrogels. As with the poly(MPC) hydrogels, the thermograms of the poly(Me(EG)$_4$MA) and poly(Me(EG)$_8$MA) hydrogels yielded single endothermic peak due to the melting of freezable water. In all the hydrogels, no other thermal transitions were observed during the heating experiments. In accordance with the earlier studies on hydrated polymer materials [17,26], the single endothermic peak observed for each hydrogel was broad toward the low-temperature side, which was in contrast to that for bulk water. This results from the distribution of the melting temperature of freezable water in the hydrogels [27].

From the area of each single peak, we estimated the enthalpy change (ΔH_f) associated with the melting of freezable water in the hydrogels. The values of ΔH_f for the poly(MPC), poly(Me(EG)$_4$MA), and poly(Me(EG)$_8$MA) hydrogels are plotted as a function of EWC in

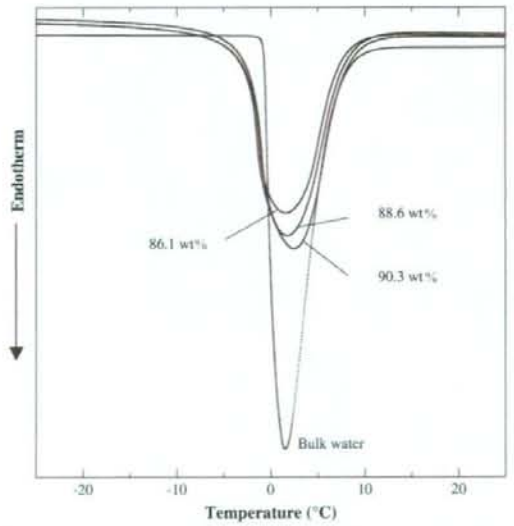

Fig. 3. DSC thermograms at a heating rate of 5 °C/min for the poly(MPC) hydrogels with different EWCs and for bulk water. The values indicated in the figure show the EWCs.

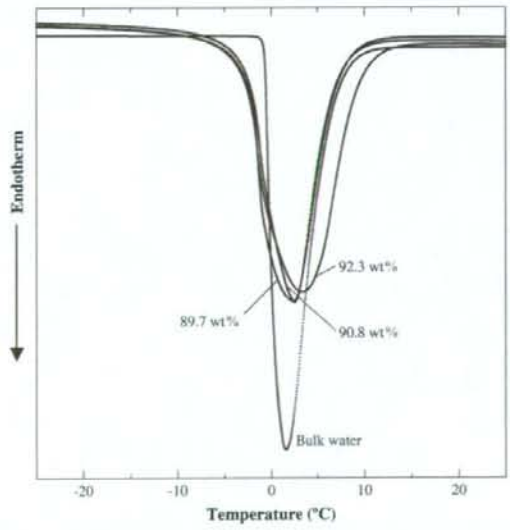

Fig. 5. DSC thermograms at a heating rate of 5 °C/min for the poly(Me(EG)$_8$MA) hydrogels with different EWCs and for bulk water. The values indicated in the figure show the EWCs.

Fig. 6. The values were less than those estimated on the supposition that all the water contained in the hydrogels behave as freezable water, which indicated that a certain amount of water in the hydrogels was unable to freeze. From the ΔH_f values, the amounts of freezable and nonfreezable water in the hydrogels can be calculated. The weight ($W_{freezable}$) of freezable water relative to that of the polymer in a hydrogel is expressed by

$$W_{freezable} = \frac{w_{freezable}}{w_{polymer}} \quad (2)$$

where $w_{freezable}$ and $w_{polymer}$ are the weight percents of freezable water and polymer in the hydrogel, respectively. Since the weight percent ($w_{nonfreezable}$) of nonfreezable water in a hydrogel is the difference between the total water content, namely EWC, and $w_{freezable}$, the weight ($W_{nonfreezable}$) of nonfreezable water relative to that of the polymer in a hydrogel is given by

$$W_{nonfreezable} = \frac{w_{nonfreezable}}{w_{polymer}} = \frac{EWC - w_{freezable}}{w_{polymer}} \quad (3)$$

Here, $w_{freezable}$ can be experimentally obtained by using ΔH_f and can be expressed by the following equation:

$$w_{freezable} = \frac{\Delta H_f}{\Delta H_w} \times 100 \quad (4)$$

where ΔH_f is the enthalpy change associated with the melting of freezable water per weight of a hydrogel and ΔH_w is the enthalpy change for the melting of bulk water. On the basis of Eq. (4), Eqs. (2) and (3) can be rewritten as

$$W_{freezable} = \frac{1}{w_{polymer}}\left(\frac{\Delta H_f}{\Delta H_w} \times 100\right) \quad (5)$$

$$W_{nonfreezable} = \frac{1}{w_{polymer}}\left(EWC - \frac{\Delta H_f}{\Delta H_w} \times 100\right) \quad (6)$$

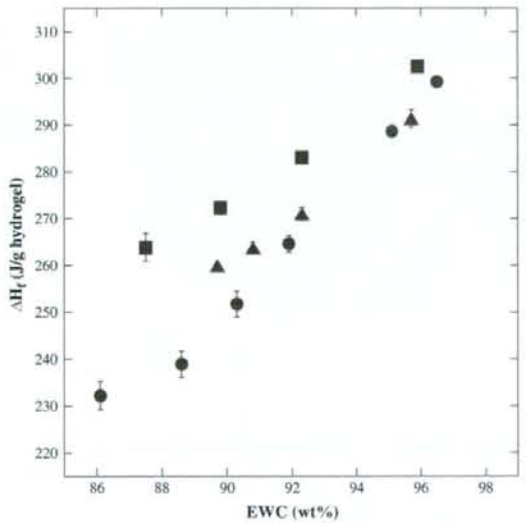

Fig. 6. Enthalpy changes associated with the melting of freezable water in the hydrogels as a function of EWC: poly(MPC) (●), poly(Me(EG)$_4$MA) (■), and poly(Me(EG)$_8$MA) (▲) hydrogels. The plotted values are relative to the weight of each hydrogel and were the average of four measurements. The standard deviation is used as the range of errors in the values.

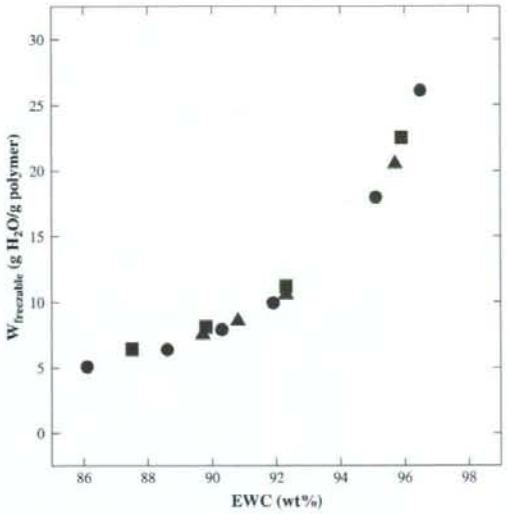

Fig. 7. Weight of freezable water relative to that of the polymer in the hydrogels as a function of EWC: poly(MPC) (●), poly(Me(EG)$_4$MA) (■), and poly(Me(EG)$_8$MA) (▲) hydrogels. The plotted values are the average of four measurements, and the standard deviation is used as the range of errors in the values.

ΔH_w measured for the distilled water used in this study was 327.5 ± 1.4 J/g (mean ± S.D., $n = 4$), which is almost the same value of bulk water (333.5 J/g). The measured ΔH_w value was used in Eqs. (5) and (6).

The $W_{freezable}$ and $W_{nonfreezable}$ values for the poly(MPC), poly(Me(EG)$_4$MA), and poly(Me(EG)$_8$MA) hydrogels are plotted as a function of EWC in Figs. 7 and 8, respectively. In Fig. 7, no significant differences were observed in the comparison of the $W_{freezable}$ values for the given values of EWC between the three

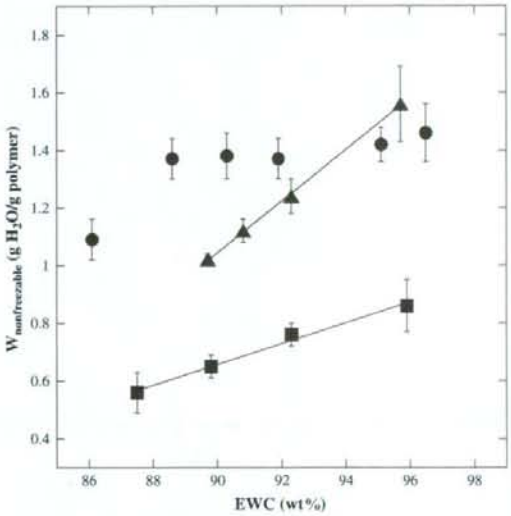

Fig. 8. Weight of nonfreezable water relative to that of the polymer in the hydrogels as a function of EWC: poly(MPC) (●), poly(Me(EG)$_4$MA) (■), and poly(Me(EG)$_8$MA) (▲) hydrogels. The plotted values are the average of four measurements, and the standard deviation is used as the range of errors in the values.

types of hydrogels. However, this result does not indicate that the amount of freezable water in the three types of hydrogels depends on the EWC. As seen in Fig. 6, the ΔH_f values for the given values of EWC differed between the hydrogels, especially in the EWC range from 86 to 92 wt%. According to Eq. (4), this difference remarkably influences the $w_{freezable}$ values. Among the hydrogels, the $w_{freezable}$ values for the given values of EWC clearly decreased in the order corresponding to poly(Me(EG)$_4$MA), poly(Me(EG)$_8$MA), and poly(MPC) hydrogels. By transforming the $w_{freezable}$ values into $W_{freezable}$ values using Eq. (5), little differences in the $W_{freezable}$ values among the hydrogels with similar EWC could be seen.

In contrast, the $W_{nonfreezable}$ values showed the large differences between the hydrogels. As shown in Fig. 8, the $W_{nonfreezable}$ values for the poly(MPC) hydrogels increased from 1.09 to 1.37 g H_2O/g polymer when the EWC was increased from 86.1 to 88.6 wt%. Moreover, the values did not change significantly (1.37–1.46 g H_2O/g polymer) with the increase in the EWC. On the other hand, the $W_{nonfreezable}$ values for the poly(Me(EG)$_4$MA) and poly(Me(EG)$_8$MA) hydrogels linearly increased with the EWC. For the poly(Me(EG)$_4$MA) hydrogels, the $W_{nonfreezable}$ values changed from 0.56 to 0.86 g H_2O/g polymer, whereas the changes in the $W_{nonfreezable}$ values for the poly(Me(EG)$_8$MA) hydrogels were from 1.02 to 1.56 g H_2O/g polymer. The poly(MPC) hydrogels showed higher $W_{nonfreezable}$ values as compared with the poly(Me(EG)$_4$MA) and poly(Me(EG)$_8$MA) hydrogels, except for the values comparable with the poly(Me(EG)$_8$MA) hydrogels when the EWC was above 95 wt%. This shows the higher hydrating ability of the poly(MPC) chains than that of the poly(Me(EG)$_4$MA) and poly(Me(EG)$_8$MA) chains. In addition, the $W_{nonfreezable}$ values for the poly(MPC) hydrogels were higher than those for protein- or polysaccharide-based materials, which have often been used as biomaterials, for similar total water contents [28–30]. It should be noted that the $W_{nonfreezable}$ values for the poly(MPC) hydrogels were constant with regard to the EWC, while those for the poly(Me(EG)$_4$MA) and poly(Me(EG)$_8$MA) hydrogels linearly increased with the EWC. We think that this feature may be related to the overlap of the hydration shells of polymer chains. In general, as the EWC of polymer hydrogels is decreased, the entanglement of polymer chains is enhanced. This leads to a decrease in the space among polymer chains. Here, the hydration shells of polymer chains overlap when the chains are mutually at some distance [31]. The constant $W_{nonfreezable}$ values for the poly(MPC) hydrogels might be caused by the absence of the overlap of the hydration shells.

Finally, we discussed the origin of nonfreezable water around poly(MPC) chains. The $W_{nonfreezable}$ values for poly(MPC) chains were transformed into the number (N_w) of nonfreezable water molecules per poly(MPC) repeating unit by the following equation:

$$N_w = W_{nonfreezable} \times \frac{M_p}{M_w} \quad (7)$$

where M_p is the molecular weight per polymer repeating unit ($M_p = 295$ for poly(MPC)) and M_w is the molecular weight of water. The results are summarized in Table 1. The N_w value per poly(MPC) repeating unit was 23–24. The phosphorylcholine groups in poly(MPC) chains are bulky and hydrophilic, so they have the large hydration capacity. Also, the value was consistent with the number of water molecules associated with each phosphorylcholine group in dodecylphosphorylcholine surfactants below the critical micelle concentration, that is, 24–25 [32]. As represented by the interaction with PEG chains of water, the formation of nonfreezable water in polymer–water systems has frequently been explained as a result of the hydrogen bonds between water molecules and polymer chains [17,26,28]. However, poly(MPC) chains have difficulty in the formation of the 23–24 nonfreezable water molecules by only the hydrogen bonds with water molecules because the primary atoms that can form hydrogen bonds with water molecules are one carbonyl oxygen and two non-ester phosphate oxygens per repeating unit. A possible explanation for the origin of nonfreezable water molecules around poly(MPC) chains may be the weak electrostatic interaction of water molecules with zwitterionic groups in phosphorylcholine groups. Kitano et al. showed that poly(MPC) chains did not significantly disturb the hydrogen bonds between their surrounding water molecules, suggesting that the phosphorylcholine groups may counteract the electrostatic hydration [33,34]. It is clear that further study is needed to characterize the origin of the nonfreezable water molecules. We believe that it can be achieved by NMR relaxation time measurements or vibrational spectroscopy such as infrared and Raman, since these methods can probe the faster motion of water networks than thermal analysis and especially, vibrational spectroscopy can provide information on local water networks.

Table 1
Number (N_w) of nonfreezable water molecules per poly(MPC) repeating unit

EWC (wt%)	96.5	95.1	91.9	90.3	88.6	86.1
N_w[a]	24 ± 2	23 ± 1	23 ± 1	23 ± 1	23 ± 1	18 ± 1

[a] The values were obtained by averaging the results of four measurements, and the standard deviation was used as the range of errors in these values.

4. Conclusion

Hydration of poly(MPC) chains was investigated by using chemically cross-linked poly(MPC) hydrogels in the EWC range from 86.1 to 96.5 wt%. It was compared with that of poly(Me(EG)$_4$MA) and poly(Me(EG)$_8$MA) chains with a similar hydration level. From the results of the enthalpy change associated with the ice-to-water transitions in the hydrogels obtained by DSC measurements, poly(MPC) chains had a higher amount of nonfreezable water than poly(Me(EG)$_4$MA) and poly(Me(EG)$_8$MA) chains. The high hydrating ability of poly(MPC) chains was kept at a high level in the EWC range. In addition, it was suggested that nonfreezable water around poly(MPC) chains was derived from electrostatic interaction as well as hydrogen bonds. It has been observed that poly(MPC) chains resist platelet adhesion and protein denaturalization for longer periods than OEG-monomethacrylate polymer and PEG chains. Thus, the results in this study may indicate that the nonfreezable water around polymer chains detected by thermal analysis may be one of the promising parameters for considering a longer duration of resistance against the protein adsorption. This study is our starting point for the establishment of hydration parameters that can characterize the relationship between the outcome of protein adsorption resistance and hydration of materials.

Acknowledgement

A part of this research was supported by the Core Research for Evolution Science and Technology (CREST) from Japan Science and Technology Agency.

References

[1] Ratner BD, Hoffman FJ, Schoen JE, Lemos F. Biomaterials science. An introduction to materials in medicine. New York: Academic Press; 1996.
[2] Chen CS, Mrksich M, Huang S, Whitesides GM, Ingber DE. Science 1997;276:1425–8.
[3] Santini JT, Cima MJ, Langer R. Nature 1999;397:335–8.
[4] Park J, Kurosawa S, Watanabe J, Ishihara K. Anal Chem 2004;76:2649–55.
[5] Brash JL. J Biomater Sci Polym Ed 2000;11:1135–46.
[6] Kenausis GL, Vörös J, Elbert DL, Huang N, Hofer R, Ruiz-Taylor L, et al. J Phys Chem B 2000;104:3298–309.
[7] Chen S, Zheng J, Li L, Jiang S. J Am Chem Soc 2005;127:14473–8.
[8] Feng W, Zhu S, Ishihara K, Brash JL. Biointerphases 2006;1:50–60.
[9] Sigal GB, Mrksich M, Whitesides GM. J Am Chem Soc 1998;120:3464–73.
[10] Vogler EA. Adv Colloid Interface Sci 1998;74:69–117.

[11] Ostuni E, Chapman RG, Holmlin RE, Takayama S, Whitesides GM. Langmuir 2001;17:5605–20.
[12] Nagaoka S, Mori Y, Takiuchi H, Yokota K, Tanzawa H, Nishiumi S. Interaction between blood components and hydrogels with poly(oxyethylene) chains. In: Shalaby SW, editor. Polymers as biomaterials. New York: Plenum Press; 1984. p. 361–74.
[13] Jeon SI, Lee JH, Andrade JD, de Gennes PG. J Colloid Interface Sci 1991; 142:149–58.
[14] Prime KL, Whitesides GM. J Am Chem Soc 1993;115:10714–21.
[15] Holmlin RE, Chen X, Chapman RG, Takayama S, Whitesides GM. Langmuir 2001;17:2841–50.
[16] Morra M. Water in biomaterials surface science. Chichester: John Wiley & Sons; 2001.
[17] Antonsen KP, Hoffman AS. Water structure of PEG solutions by differential scanning calorimetry measurement. In: Harris JM, editor. Poly(ethylene glycol) chemistry: biotechnical and biomedical applications. New York: Plenum Press; 1992. p. 15–28.
[18] Wang RLC, Kreuzer HJ, Grunze M. J Phys Chem B 1997;101:9767–73.
[19] Wang RY, Himmelhaus M, Fick J, Herrwerth S, Eck W, Grunze M. J Chem Phys 2005;122:164702–6.
[20] Ishihara K, Ueda T, Nakabayashi N. Polym J 1990;22:355–60.
[21] Iwasaki Y, Ishihara K. Anal Bioanal Chem 2005;381:534–46.
[22] Watanabe J, Ishihara K. Colloids Surf B 2008;65:155–65.
[23] Ishihara K, Iwasaki Y, Ebihara S, Shindo Y, Nakabayashi N. Colloids Surf B 2000;18:325–35.
[24] Ishihara K. The role of water in the surface properties of phospholipid polymers. In: Morra M, editor. Water in biomaterials surface science. Chichester: John Wiley & Sons; 2001. p. 333–51.
[25] Kiritoshi Y, Ishihara K. J Biomater Sci Polym Ed 2002;13:213–24.
[26] Huang L, Nishinari K. J Polym Sci Part B Polym Phys 2001;39:496–506.
[27] Kuntz ID, Kauzmann W. Adv Protein Chem 1974;28:239–345.
[28] Joshi HN, Topp EM. Int J Pharm 1992;80:213–25.
[29] Liu WG, Yao KD. Polymer 2001;42:3943–7.
[30] Megeed Z, Cappello J, Ghandehari H. Biomacromolecules 2004;5:793–7.
[31] Kjellander R, Florin E. J Chem Soc Faraday Trans 1 1981;77:2053–77.
[32] Yaseen M, Lu JR, Webster JRP, Penfold J. Langmuir 2006;22:5825–32.
[33] Kitano H, Sudo K, Ichikawa K, Ide M, Ishihara K. J Phys Chem B 2000;104:11425–9.
[34] Kitano H, Imai M, Mori T, Gemmei-Ide M, Yokoyama Y, Ishihara K. Langmuir 2003;19:10260–6.

FULL PAPER *Surgery*

Prevention of Biofilm Formation with a Coating of 2-Methacryloyloxyethyl Phosphorylcholine Polymer

Kiyohisa FUJII[1], Hiroko N. MATSUMOTO[1], Yoshihisa KOYAMA[1], Yasuhiko IWASAKI[1], Kazuhiko ISHIHARA[2] and Kazuo TAKAKUDA[1]*

[1]*Institute of Biomaterials and Bioengineering, Tokyo Medical and Dental University, 2–3–10 Kanda-Surugadai, Chiyoda-ku, Tokyo 101–0062 and* [2]*Department of Materials Engineering, School of Engineering, The University of Tokyo, 7–3–1 Hongou, Bunkyou-ku, Tokyo 113–8656, Japan*

(Received 27 June 2007/Accepted 19 October 2007)

ABSTRACT. Device-associated infections are serious complications, and their prevention is an issue of considerable importance. Since biofilms are responsible for these refractory infections, effective methods to inhibit biofilm formation are required. In this investigation, stainless steel plates with and without 2-methacryloyloxyethyl phosphorylcholine (MPC) polymer, i.e., poly (MPC-co-n-butyl methacrylate) (PMB) coating, were incubated in a medium containing bacteria. In the course of incubation, half of the specimens received antibiotics. The specimens were stained for nucleic acid and polysaccharides, and then examined with a confocal laser scanning microscope. The numbers of bacteria on the specimen surfaces were evaluated by an ATP assay. On the surfaces of the specimens without PMB coating, the formation of a biofilm enveloping bacteria was confirmed. The addition of antibiotics did not effectively decrease the number of bacteria. On the other hand, on the surfaces of the specimens with PMB coating, no biofilm formation was observed, and the number of bacteria was significantly decreased. The addition of potent antibiotics further decreased the number of bacteria by 1/100 to 1/1000 times. The PMB coating combined with the validated use of antibiotics might provide a method for the simultaneous achievement of biocompatible surfaces of devices and the prevention of device-associated infections.

KEY WORDS: biofilm, biomaterials, device-associated infection, MPC, PMB coating.

J. Vet. Med. Sci. 70(2): 167–173, 2008

Device-associated infections are serious complications in patients receiving indwelling catheters. These complications, however, do not limited in such cases; device-associated infections are consistent risk accompanying the usage of any artificial devices. For instance, applications of bone fixation plates to open fractures are contraindicated. Actually, the rate of the infections was reported to be as high as 15% to 18% [23] if an aseptic condition was not maintained during the treatment. Although the microorganisms responsible for these infections are usually indigenous bacteria such as *Staphylococcus epidermidis*, a difficulty arises as antibacterial agents are not effective against these infections. Once the infections are established, persistent inflammations continue as long as the devices remain in the body.

Device-associated infections are caused by bacteria that adhere to the surfaces of internal prosthetic devices and are thought to develop through the following sequence of events [3, 7, 10, 18, 22]. Immediately after the implantation of devices into patients, various molecules such as peptides and proteins are adsorbed onto the surfaces of the materials. These molecules mediate the attachment of bacteria. Once the bacteria, e.g., those belonging to the species *S. epidermidis*, are attached to the surfaces of devices, they proliferate and aggregate there to form biofilms in which the bacteria are enveloped in a thin layer of polysaccharides. The bacteria in the biofilms are protected from the biological defense mechanism, including phagocytosis by macrophages and immunological responses, as well as antibacterial agents for therapeutic use. Hence, the formation of biofilms on the surface of devices establishes refractory infections, i.e., device-associated infections [6, 8, 19, 24, 27, 28].

Various strategies were proposed and are expected to be effective in preventing device-associated infections. Wassall [31] utilized silver coating on stainless steel pins for external skeletal fixation and reported successful infection control. Takahashi [29] developed antibacterial catheters coated with citrate silver and lecithin and reported that biofilm formations were prevented. In these reports, silver coating that has an antibacterial effect was utilized; however, silver is not a biocompatible material and might exert adverse effects on living tissues. It is desirable to realize another approach in which only biocompatible materials are utilized for preventing device-associated infections.

2-Methacryloyloxyethyl phosphorylcholine (MPC) was designed taking into account the surface structure of the biomembrane. MPC polymers have a surface that resists nonspecific protein adsorption and cell adhesion [13–17, 25]. It has been attracting considerable attention for its remarkable antithrombogenicity and has been applied successfully to artificial blood vessels, implantable artificial hearts and artificial lungs. The MPC polymer coating renders the surfaces extremely hydrophilic, prevents the adhesion of proteins, and inhibits the adhesion of platelets. Noting the similarity of platelet adhesion and bacterial adhesions, we might expect that the MPC polymer coating also leads to the inhibition of bacterial adhesion and the forma-

* CORRESPONDENCE TO: TAKAKUDA, K., Institute of Biomaterials and Bioengineering, Tokyo Medical and Dental University, 2–3–10 Kanda-Surugadai, Chiyoda-ku, Tokyo 101–0062, Japan.
e-mail: takakuda.mech@tmd.ac.jp

tion of biofilm. In fact, Hirota *et al.* [9] had coated coverslips made of polyethylenetelephthalate with MPC polymer and observed decreased adhesion of bacteria to the coverslip surfaces. In their experiments, however, they exposed the specimens to bacteria for only 1 hr and counted the number of bacteria attached to the specimens during this period. In order to elucidate whether MPC polymer coating prevents biofilm formation, a comparative study concerning biofilm formation on noncoated and MPC polymer-coated surfaces, which requires a longer period of exposure to bacteria, should be conducted. Hence, in this investigation, we carried out biofilm formation experiments with both surfaces and examined how MPC polymer, i.e., poly[MPC-co-n-butyl methacrylate (BMA)] (PMB) coating inhibits the formation of biofilms.

MATERIALS AND METHODS

Plate specimens: Stainless steel plates (SUS316L; Nilaco Corp., Tokyo, Japan) with a thickness of 0.1 mm and dimensions of 5 × 5 × 0.1 mm were prepared. The composition of this material was standardized for medical use such as bone fixation devices. Since surface characteristics as bacterial adhesion were examined in this experiment, thin plates of 0.1-mm thickness were adopted for the sake of convenience in cultivation. The specimens were cleaned with acetone, washed with distilled water, and autoclaved at 121°C for 20 min. Further operations with the specimens were carried out in sterile conditions.

Coating with MPC polymer: The MPC was synthesized as previously reported [14]. The PMB was synthesized by radical polymerization of desired amount of MPC and n-butyl methacrylate in ethanol using 2,2'-azobisisobutyronitrile (AIBN) as an initiator [16]. The chemical structure of the PMB was determined by ^{1}H-NMR and IR spectroscopies. The composition of the MPC unit was 30 mol%. The structural formula of PMB [12] is illustrated in Fig. 1. The PMB was resolved in ethanol, and the concentration was adjusted to 0.5% (wt/vol). The stainless steel specimens were immersed in the PMB solution and then dried on a clean bench. Before the specimens thus coated with PMB were used in culture experiments, they were immersed in calcium- and magnesium-free phosphate-buffered saline (PBS(–), pH 7.2)) for 30 min.

Bacterial preparation: *Staphylococcus aureus* (JCM 2151), *S. epidermidis* (JCM 2414), and *Pseudomonas aeruginosa* (JCM 2412) were purchased from Japan Collection of Microorganisms (Riken BioResource Center, Wako, Japan) and utilized in this investigation.

Cultivation experiments for confocal laser scanning microscope (CLSM) observation: Organisms were grown in the culture medium reported by Akiyama *et al.* [1], that was soybean-casein digest broth (Nihon Pharm., Tokyo, Japan) supplemented with the same amount of normal rabbit plasma (Denka Seiken, Tokyo, Japan). Cultivation experiments were performed following the previous reports [1, 9, 11, 27, 30]. Briefly, the specimen was placed on a 35-mm culture dish, and 2.0 m*l* of the culture medium containing bacteria was added. The concentration of bacteria was 3 × 10^8 cells/m*l*. The dish thus prepared was kept in an incubator at 37°C for 48 hr, and the observations of the specimens with a confocal scanning microscope were then performed.

Cultivation experiments for ATP assay: As was done in the cultivation experiments, the specimen was cultured in a 35-mm dish for 24 hr with the medium containing bacteria at a concentration 3 × 10^8 cells/m*l*. Subsequently, we took out the specimen from the dish and rinse away the medium with PBS(–). Then the specimen was transferred to another dish, and 2.0 m*l* of the culture medium supplemented with or without antibiotics was added. The antimicrobial agents were used to investigate the antibiotic resistance of the bacteria enveloped in the biofilm. The specimens were further incubated for another 24 hr in the incubator. The antibiotics utilized were either cefazolin sodium salt (100 μg/m*l*; Fujisawa, Osaka, Japan) or gentamicin sulfate (50 μg/m*l*; MP Biomedicals, Aurora, OH, U.S.A.). In the preparatory experiment, susceptibility of the bacteria to the antibiotics had been examined with the disk diffusion method [5]. We had observed a circular zone of inhibition surrounding a paper disk impregnated with gentamicin for all cases of *S. aureus, S. epidermidis*, and *P. aeruginosa*. On the other hand, a zone of inhibition surrounding cefazolin was resulted for *S. aureus* and *S. epidermidis* but not for *P. aeruginosa*. Hence the bacteria used in this experiment were susceptible to the utilized antibiotics, except the case of *P. aeruginosa* to cefazolin.

CLSM observations: The formation of biofilm was confirmed by the observation with a CLSM [1, 2, 4, 26, 30].

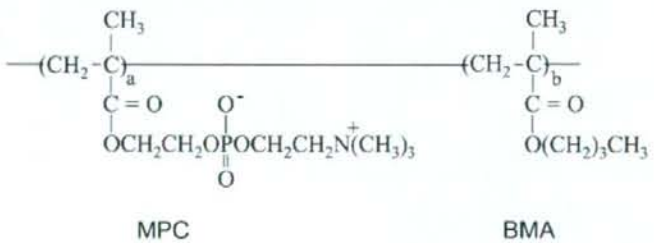

Fig. 1. Chemical formula of poly [MPC-co-n-butyl methacrylate (BMA)] (PMB) used in this study.